from a *de novo* assembly of Berok (generated using Roche GS Assembler version 2.6, with 40-bp minimum overlap, 90% identity) to the B strain using the Burrows-Wheeler Aligner (BWA)[37] and allowing for gaps. Using the Phred-scaled probability of the base being misaligned by SAMtools[35], indel candidates were called from the alignment. In-house Python scripts were used to then cross-reference with the microsatellites found in the reference strain B assembly identified by MISA (see URLs). All homopolymer microsatellites were discarded to account for potential sequence errors introduced by 454 sequencing.

Selective constraint analysis of 4,563 orthologs between *P. cynomolgi* strains B and Berok and 4,601 orthologs between these strains and *P. vivax* Salvador I used MUSCLE[38] alignments with stringent removal of gaps and missing data (*P. cynomolgi* Berok orthologs were identified through a reciprocal best-hit BLAST search against strain B genes). Analyses were conducted using the Nei-Gojobori model[25]. To detect values that could not be explained by chance, we estimated the standard error by a bootstrap procedure with 200 pseudoreplicates for each gene. The expected value for d_S/d_N is 0 if a given pair of sequences is diverging without obvious effects on fitness. In the case of the comparison within *P. cynomolgi*, values with a difference of ± 2 s.e.m. from 0 were considered indicative of an excess of synonymous ($d_S/d_N > 0$) or nonsynonymous ($d_S/d_N < 0$) changes. In the case of the comparison between *P. cynomolgi* and *P. vivax*, we used a more stringent criterion of ± 3 s.e.m. from 0.

28. Ohtsubo, Y., Ikeda-Ohtsubo, W., Nagata, Y. & Tsuda, M. GenomeMatcher: a graphical user interface for DNA sequence comparison. *BMC Bioinformatics* **9**, 376 (2008).
29. Cantarel, B.L. *et al.* MAKER: an easy-to-use annotation pipeline designed for emerging model organism genomes. *Genome Res.* **18**, 188–196 (2008).
30. Popendorf, K., Tsuyoshi, H., Osana, Y. & Sakakibara, Y. Murasaki: a fast, parallelizable algorithm to find anchors from multiple genomes. *PLoS ONE* **5**, e12651 (2010).
31. Thompson, J.D., Higgins, D.G. & Gibson, T.J. CLUSTAL W: improving the sensitivity of progressive multiple sequence alignment through sequence weighting, position-specific gap penalties and weight matrix choice. *Nucleic Acids Res.* **22**, 4673–4680 (1994).
32. Felsenstein, J. *PHYLIP, Phylogeny Inference Package*, 3.6a3 edn (University of Washington, Seattle, 2005).
33. Yang, Z. PAML 4: phylogenetic analysis by maximum likelihood. *Mol. Biol. Evol.* **24**, 1586–1591 (2007).
34. Ning, Z., Cox, A.J. & Mullikin, J.C. SSAHA: a fast search method for large DNA databases. *Genome Res.* **11**, 1725–1729 (2001).
35. Li, H. A statistical framework for SNP calling, mutation discovery, association mapping and population genetical parameter estimation from sequencing data. *Bioinformatics* **27**, 2987–2993 (2011).
36. Tamura, K., Dudley, J., Nei, M. & Kumar, S. MEGA4: Molecular Evolutionary Genetics Analysis (MEGA) software version 4.0. *Mol. Biol. Evol.* **24**, 1596–1599 (2007).
37. Li, H. & Durbin, R. Fast and accurate short read alignment with Burrows-Wheeler transform. *Bioinformatics* **25**, 1754–1760 (2009).
38. Edgar, R.C. MUSCLE: multiple sequence alignment with high accuracy and high throughput. *Nucleic Acids Res.* **32**, 1792–1797 (2004).

Virology 432 (2012) 29–38

Contents lists available at SciVerse ScienceDirect

Virology

journal homepage: www.elsevier.com/locate/yviro

Trans-complemented hepatitis C virus particles as a versatile tool for study of virus assembly and infection

Ryosuke Suzuki [a,*], Kenji Saito [a], Takanobu Kato [a], Masayuki Shirakura [b], Daisuke Akazawa [a], Koji Ishii [a], Hideki Aizaki [a], Yumi Kanegae [c], Yoshiharu Matsuura [d], Izumu Saito [c], Takaji Wakita [a], Tetsuro Suzuki [e,**]

[a] *Department of Virology II, National Institute of Infectious Diseases, 1-23-1 Toyama, Shinjuku-ku, Tokyo 162-8640, Japan*
[b] *Influenza Virus Research Center, National Institute of Infectious Diseases, Tokyo 208-0011, Japan*
[c] *Institute of Medical Science, University of Tokyo, Tokyo 108-8639, Japan*
[d] *Research Institute for Microbial Diseases, Osaka University, Osaka 565-0871, Japan*
[e] *Department of Infectious Diseases, Hamamatsu University School of Medicine, 1-20-1 Handayama, Higashi-ku, Hamamatsu, Shizuoka 431-3192, Japan*

ARTICLE INFO

Article history:
Received 30 March 2012
Returned to author for revisions
23 April 2012
Accepted 25 May 2012
Available online 22 June 2012

Keywords:
HCV
HCVtcp
Trans-packaging
Single-round infection

ABSTRACT

In this study, we compared the entry processes of *trans*-complemented hepatitis C virus particles (HCVtcp), cell culture-produced HCV (HCVcc) and HCV pseudoparticles (HCVpp). Anti-CD81 antibody reduced the entry of HCVtcp and HCVcc to almost background levels, and that of HCVpp by approximately 50%. Apolipoprotein E-dependent infection was observed with HCVtcp and HCVcc, but not with HCVpp, suggesting that the HCVtcp system is more relevant as a model of HCV infection than HCVpp. We improved the productivity of HCVtcp by introducing adapted mutations and by deleting sequences not required for replication from the subgenomic replicon construct. Furthermore, blind passage of the HCVtcp in packaging cells resulted in a novel mutation in the NS3 region, N1586D, which contributed to assembly of infectious virus. These results demonstrate that our plasmid-based system for efficient production of HCVtcp is beneficial for studying HCV life cycles, particularly in viral assembly and infection.

Introduction

Over 170 million people worldwide are chronically infected with hepatitis C virus (HCV), and are at risk of developing chronic liver diseases (Hoofnagle, 2002). HCV is an enveloped virus of the family *Flaviviridae*, and its genome is a positive-strand RNA consisting of the 5′-untranslated region (UTR), an open reading frame encoding viral proteins (core, E1, E2, p7, NS2, NS3, NS4A, NS4B, NS5A, and NS5B) and the 3′-UTR (Suzuki et al., 2007).

Host–virus interactions are required during the initial steps of viral infection. It was previously reported that CD81 (Bartosch et al., 2003a, b; McKeating et al., 2004; Pileri et al., 1998), scavenger receptor class B type I (Bartosch et al., 2003a, b; Scarselli et al., 2002), claudin-1 (Evans et al., 2007; Liu et al., 2009) and occludin (Benedicto et al., 2009; Evans et al., 2007; Liu et al., 2009; Ploss et al., 2009) are critical molecules for HCV entry into cells. CD81 interacts with HCV E2 via a second extracellular loop (Bartosch et al., 2003a, b; Hsu et al., 2003) and its role in the internalization process was confirmed (Cormier et al., 2004; Flint et al., 2006). It has also been shown that infectious HCV particles produced in cell cultures (HCVcc) exist as apolipoprotein E (ApoE)-enriched lipoprotein particles (Chang et al., 2007) and that ApoE is important for HCV infectivity (Owen et al., 2009).

Investigation of HCV had been hampered by difficulties in amplifying the virus in vitro before development of robust cell culture systems based on JFH-1 isolates (Lindenbach et al., 2005; Wakita et al., 2005; Zhong et al., 2005). Retrovirus-based HCV pseudoparticles (HCVpp), in which cell entry is dependent on HCV glycoproteins, have been used to study virus entry (Bartosch et al., 2003a; Hsu et al., 2003). Vesicular stomatitis virus (VSV)-based pseudotypic viruses bearing HCV E1 and E2 and replication-competent recombinant VSV encoding HCV envelopes have also been available as surrogate models for studies of HCV infection (Mazumdar et al., 2011; Tani et al., 2007).

It was recently shown that HCV subgenomic replicons can be packaged when structural proteins are supplied in *trans* (Adair et al., 2009; Ishii et al., 2008; Masaki et al., 2010; Steinmann et al., 2008). These *trans*-complemented HCV particles (HCVtcp) are infectious, but support only single-round infection and are unable to spread. Establishment of flexible systems to efficiently produce HCVtcp should contribute to studying HCV assembly, in particular encapsidation of the viral genome, and entry to cells with less stringent biosafety and biosecurity measures. Although single-round infection can be achieved by using the HCVcc system with receptor knock-out

* Corresponding author. Fax: +81 3 5285 1161.
** Corresponding author. Fax: +81 53 435 2338.
E-mail addresses: ryosuke@nih.go.jp (R. Suzuki), tesuzuki@hama-med.ac.jp (T. Suzuki).

0042-6822/$ - see front matter © 2012 Elsevier Inc. All rights reserved.
http://dx.doi.org/10.1016/j.virol.2012.05.033

cells, the single-round HCVcc system is not suitable for studying virus entry. We previously described plasmid-based production of HCVcc and HCVtcp (Masaki et al., 2010). Here, we demonstrated that HCVtcp production can be enhanced by introducing the previously reported cell-culture adaptive mutations and by deleting sequences not essential for replication in the subgenomic replicon construct. By providing genotype 1b-derived core-to-p7 in addition to intragenotypic viral proteins, chimeric HCVtcp were generated. Furthermore, blind passage of HCVtcp in the packaging cells resulted in the identification of a novel cell culture-adaptive mutation in NS3 that enables us to establish the efficient production of HCVtcp with structural proteins from various strains. Taken together, our system for producing single-cycle infectious HCV particles should be useful in the study of entry and assembly steps of the HCV life cycles. This technology may also have potential to be the basis for the safer vaccine development.

Results

Enhancement of HCVtcp production by adaptive mutations in E2, p7 and NS2 and by deleting sequences not essential for replication from replicon construct

In our HCVtcp system, the RNA polymerase I (Pol I)-driven replicon plasmid, which carries a dicistronic subgenomic luciferase reporter replicon of JFH-1 strain with a Pol I promoter and terminator (pHH/SGR-Luc), as well as a plasmid containing core-NS2 cDNA under the CAG promoter (pCAGC-NS2) were used (Masaki et al., 2010). In an effort to improve the yield of HCVtcp production, cell culture-adaptive mutations in E2 (N417S), p7 (N765D) and NS2 (Q1012R) which were previously selected from serial passage of HCVcc (Russell et al., 2008) were introduced into the core-NS2 expression plasmid (Fig. 1A) (residues are numbered

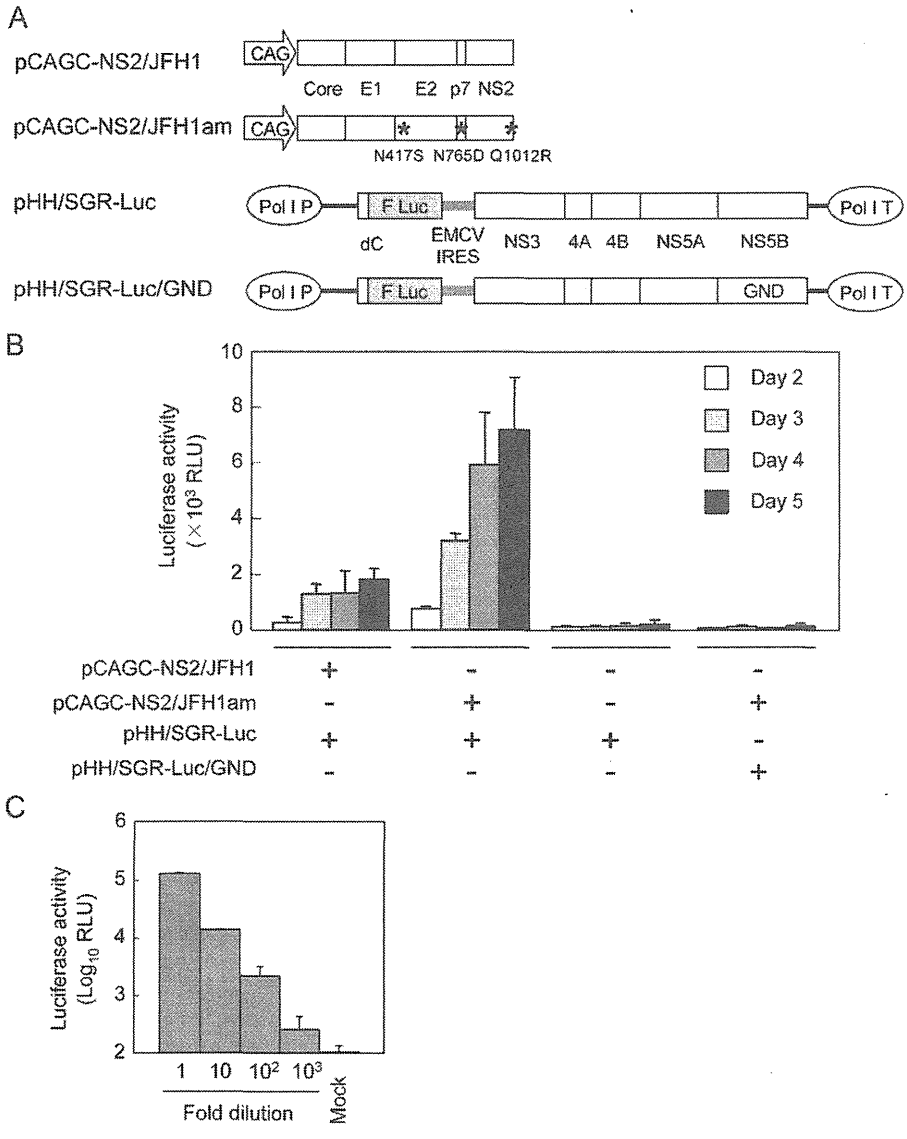

Fig. 1. HCVtcp production by two-plasmid transfection. (A) Schematic representation of plasmids is shown. HCV polyproteins derived from JFH-1 are indicated by white boxes. HCV UTRs are indicated by bold lines. The internal ribosomal entry site from encephalomyocarditis virus (EMCV IRES) is denoted as gray lines. Adaptive mutations are indicated as asterisks. F Luc: firefly luciferase gene; CAG: CAG promoter; Pol I P: RNA polymerase I promoter; Pol I T: RNA polymerase I terminator; GND: replication-deficient GND mutation. (B) Luciferase activity in Huh7.5.1 cells inoculated with supernatant from cells transfected with indicated plasmids at the indicated time points. Data are averages of triplicate values with error bars showing standard deviations. (C) Luciferase activity in cells inoculated with serially diluted HCVtcp.

according to positions within the JFH-1 polyprotein). Supernatants of cells transfected with plasmids (Fig. 1A) were collected and were used to infect Huh7.5.1 cells, which were analyzed by luciferase assay. Introduction of adaptive mutations (pCAGC-NS2/JFH1am) resulted in more than 4-fold higher production of HCVtcp at 5 day post-transfection, as compared to wild-type (WT) (pCAGC-NS2/JFH1) (Fig. 1B), indicating that the adaptive mutations contribute to enhancing HCVtcp production. To confirm that luciferase activity levels in HCVtcp-infected cells are correlated with the number of infectious particles, Huh7.5.1 cells were inoculated with serial dilutions of HCVtcp. Luciferase activity was well correlated with viral load (Fig. 1C), indicating that luciferase assay in HCVtcp-infected cells can be used to quantify HCV infection.

In order to further explore the efficient production of HCVtcp, we generated replicon constructs that lack the luciferase gene or include the partial coding sequences for structural proteins instead of reporter (Fig. 2A). Replication of each replicon in plasmid-transfected cells was then assessed by Western blotting (Fig. 2B). Among the constructs tested, NS5B levels were lowest in cells expressing pHH/SGR-Luc. NS5B levels in cells replicating other replicons appeared to be comparable. Cells were infected with supernatants of cells transfected with each replicon plasmid, along with pCAGC-NS2/JFH1am, followed by infectious unit assay (Fig. 2C). The highest production of HCVtcp was obtained from cells transfected with pHH/SGR, where the luciferase sequence was deleted from pHH/SGR-Luc, thus suggesting that deletion of the sequence not essential for RNA replication in the replicon may contribute to enhancing HCVtcp production.

Production of chimeric HCVtcp by providing heterologous core-p7

In order to elucidate whether *trans*-encapsidation of JFH-1 replicon can be achieved by providing core-p7 from other HCV strains, core-NS2 plasmids were constructed (Fig. 3A). In these plasmids, core through the N-terminal 33 aa of NS2, which contains transmembrane domain 1 of NS2, was derived from either H77c (genotype 1a), THpa (genotype 1b), Con1 (genotype 1b) or J6 (genotype 2a) strain. Residual NS2 was derived from JFH-1, as described previously (Pietschmann et al., 2006). HCVtcp was efficiently produced by core-p7 of J6 and THpa strains, but its production was less efficient in the case of Con1 strain. *Trans*-packaging was not detectable when core-p7 of H77c strain was used (Fig. 3C). Among HCV strains tested, difference in luciferase activity levels in HCVtcp-infected cells (Fig. 3C) were in agreement with that in the viral RNA levels in the culture supernatants of the transfected cells (Fig. 3B). Although the efficacy of *trans*-complementation was variable among strains, chimeric HCVtcp can be generated by providing genotype 1b-derived core-p7 in addition to intragenotypic viral proteins, and was used in subsequent studies.

ApoE- and CD81-dependent infection by HCVtcp

There is accumulating evidence that apolipoproteins, particularly ApoE, contribute to HCV production and infectivity (Chang et al., 2007; Owen et al., 2009). To determine whether ApoE is involved in infection of target cells by HCVtcp, we infected cells in the presence of increasing concentrations of anti-ApoE antibody.

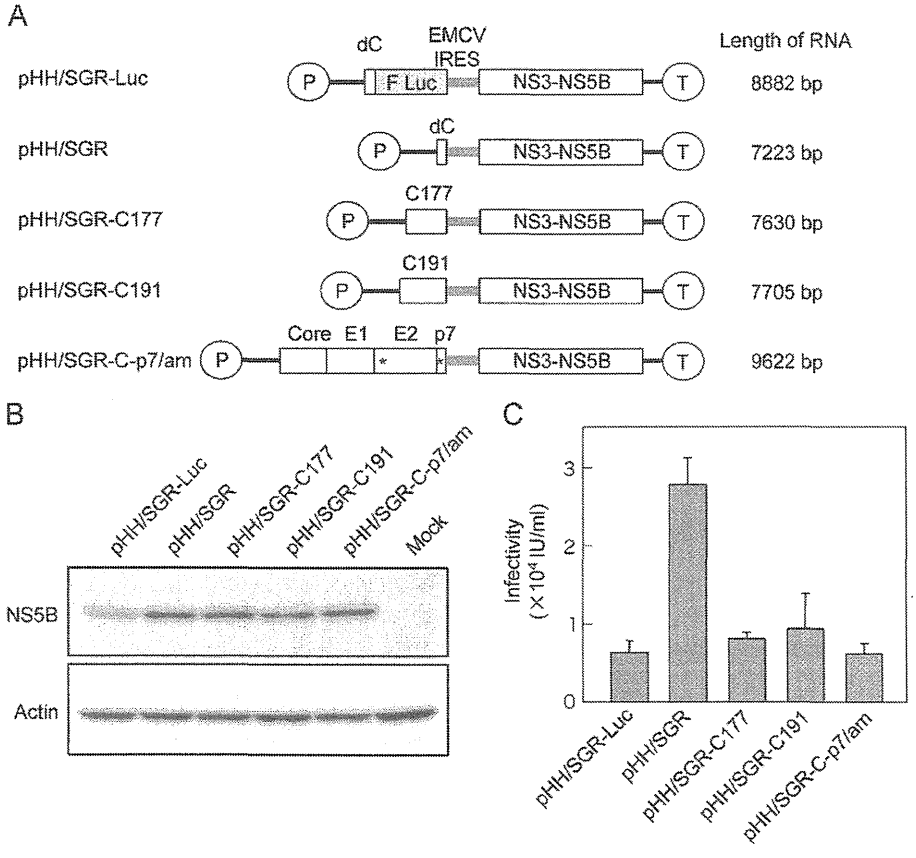

Fig. 2. Production of HCVtcp with different replicon constructs. (A) Schematic representation of plasmids used for production of HCVtcp. Deduced length of transcribed RNA from each construct is shown on the right. HCV polyproteins from JFH-1 strain are indicated by open boxes. HCV UTRs are indicated by bold lines. The EMCV IRES is denoted by gray bars. Adaptive mutations are indicated by asterisks. F Luc: firefly luciferase gene; P: RNA polymerase I promoter; T: RNA polymerase I terminator. (B) Detection of NS5B and actin in Huh7.5.1 cells transfected with indicated plasmids at 4 day post-transfection. (C) Infectivity of culture supernatants from cells transfected with indicated replicon plasmids along with pCAGC-NS2/JFH1am at 4 day post-transfection.

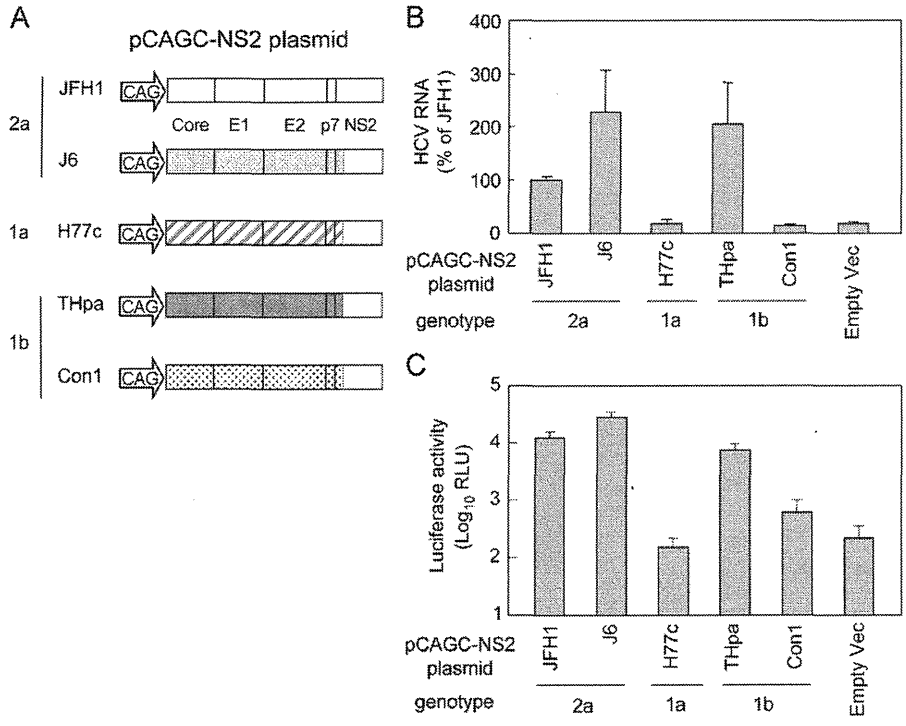

Fig. 3. HCVtcp production with structural proteins from various strains. (A) Schematic representation of plasmids used. HCV polyproteins of JFH-1, J6, H77c, THpa and Con1 strain are shown in the open box, bright gray box, box with diagonal lines, dark gray box and dotted box, respectively. (B) Relative levels of HCV RNA in the supernatant from cells transfected with indicated plasmids along with pHH/SGR-Luc. (C) Luciferase activity in cells inoculated with supernatant from cells transfected with indicated plasmids along with pHH/SGR-Luc at 4 day post-transfection.

pCAGC-NS2/THpa and pCAGC-NS2/JFH1am were used as core-NS2 plasmids for HCVtcp production carrying core-p7 derived from genotypes 1b and 2a (HCVtcp-1b and HCVtcp-2a, respectively). HCVpp derived from JFH-1 and VSVpp were generated and used for comparison. Infection with HCVtcp-1b or HCVtcp-2a was blocked by anti-ApoE antibody in a dose-dependent manner. In contrast, anti-ApoE antibody did not affect infection with HCVpp and VSVpp (Fig. 4A).

The CD81 dependence of infection was also compared between HCVtcp and HCVpp (Fig. 4B). Anti-CD81 antibody inhibited the entry of HCVtcp-1b, HCVtcp-2a, and HCVpp in a dose-dependent manner. The antibody had no effect on VSVpp infection. HCVtcp infection appears to be more sensitive to anti-CD81 antibody when compared with HCVpp infection; more than 60% inhibition was observed at 0.08 μg/mL anti-CD81 antibody for HCVtcp-1b and HCVtcp-2a, whereas approximately 50% inhibition was observed for HCVpp at 2 μg/mL antibody. Neutralization of HCVcc by anti-ApoE and anti-CD81 antibodies was also determined. Antibodies blocked HCVcc infection (Fig. 4C and D), as observed with HCVtcp. These results suggest that ApoE, as well as CD81, play an important role in HCVtcp infection. Thus, HCVtcp may be more useful for evaluating the HCV entry process than HCVpp.

Identification of novel culture-adaptive mutation in NS3 by serial passage of HCVtcp in packaging cells

The HCVtcp system was further applied to analyses of genetic changes during serial passages in target cells. As an initial attempt, supernatants of cells co-transfected with pCAGC-NS2/JFH1am and pHH/SGR were inoculated into Huh7.5.1 cells transiently transfected with pCAGC-NS2/JFH1am. However, infectious titer was lost after repeated inoculation, likely due to low HCVtcp titers and low efficiency of plasmid transduction (data not shown). To overcome this, we utilized recombinant adenovirus vectors (rAdVs) to provide core-NS2. As we were not able to obtain rAdV directly expressing core-NS2, conditional transgene expression based on a Cre-loxP strategy was employed (Kanegae et al., 1995). We constructed an rAdV containing core-NS2 gene downstream of a stuffer DNA flanked by a pair of loxP sites (AxCALNLH-CNS2). When cells were doubly infected with AxCALNLH-CNS2 and the Cre-expressing rAdV, AxCANCre (Kanegae et al., 1995), the Cre-mediated excisional deletion removed the stuffer DNA, resulting in core-NS2 expression under control of the CAG promoter (Fig. 5A). As expected, tightly regulated production of HCVtcp was observed. The cells infected with AxCANCre and AxCALNLH-CNS2 along with transduction of pHH/SGR-Luc produced HCVtcp at high levels. Production of HCVtcp was undetectable when either AxCANCre or AxCALNLH-CNS2 was not infected (Fig. 5B). The Cre-mediated rAdV expression system appears to have yielded considerably higher production of HCVtcp when compared with the settings for plasmid co-transfection.

Supernatants from cells in which core-NS2 was expressed using rAdVs and the subgenomic RNA derived from pHH/SGR replicated were inoculated into cells infected with AxCALNLH-CNS2 and AxCANCre (Fig. 6A). Blind passage was performed by sequentially transferring culture supernatants to cells infected with the above rAdVs. The two independent 10 blind passages (p10) showed virus titers of $>1\times10^6$ IU/mL, which were markedly higher than those of the passage 0 (p0) stock cultures (4×10^4 IU/mL). Side-by-side infection analysis revealed that the HCVtcp p10 #1 achieved a virus titer approximately 36 times higher than that of HCVtcp p0 on the packaging cells at 6 day post-infection (Fig. 6B). Sequencing of the entire replicon in the supernatants at p10 in two independent experiments revealed

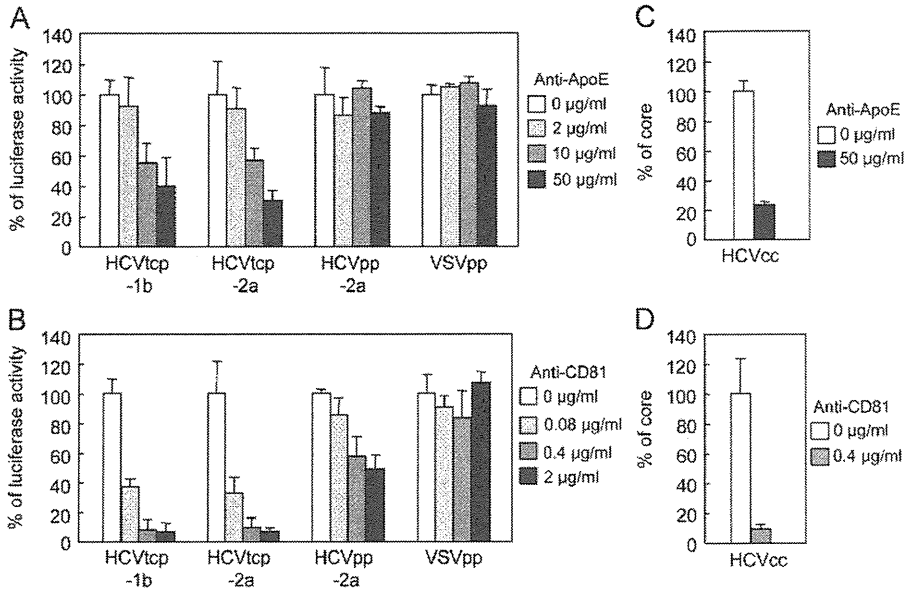

Fig. 4. Effects of anti-ApoE and anti-CD81 antibodies on HCV entry. (A) Aliquots of virus sample were incubated with increasing concentrations of anti-ApoE antibodies for 1 h and were then added to Huh7.5.1 cells. Luciferase activity was determined at 72 h post-infection and is expressed relative to activity without antibodies (white bar). (B) Huh7.5.1 cells were preincubated for 1 h with increasing concentrations of anti-CD81 antibodies, followed by inoculating virus samples. Luciferase activity was determined and expressed as shown in (A). (C) Aliquots of HCVcc were incubated with anti-ApoE antibodies for 1 h and were then added to Huh7.5.1 cells at an MOI of 0.05. Intracellular core levels were quantitated at 24 h post-infection and are expressed relative to levels without antibodies (white bar). (D) Huh7.5.1 cells were preincubated for 1 h with anti-CD81 antibodies. HCVcc infection and measurement of core proteins were performed as indicated in (C).

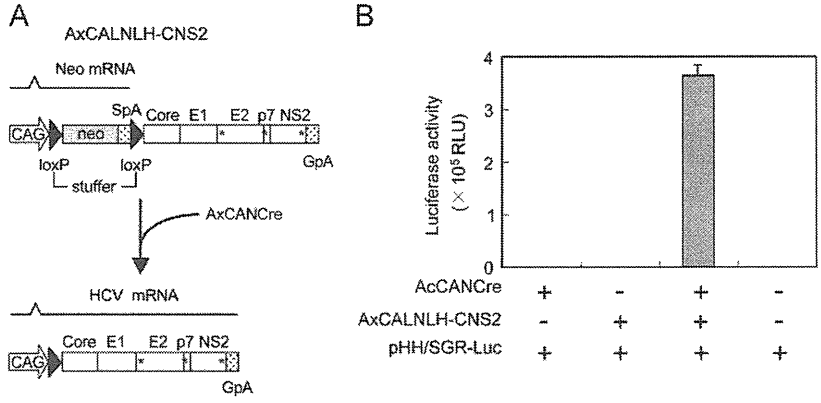

Fig. 5. Transgene activation mediated by rAdVs expressing Cre recombinase under control of CAG promoter. (A) Cre recobminase expressed by AxCANCre recognizes a pair of its target sequences loxP in AxCALNLH-CNS2, and removes the stuffer region resulting in expression of HCV core-NS2 polyprotein by CAG promoter. CAG: CAG promoter; SpA: SV40 early polyA signal; GpA: rabbit b-globin poly(A) signal. (B) Luciferase activity in Huh7.5.1 cells inoculated with 4-day post-transfection culture supernatant from cells transfected with pHH/SGR-Luc, and then infected with indicated rAdVs.

that both passaged HCVtcp had an identical nonsynonymous mutation in the NS3 region (N1586D) (Fig. 6C).

In order to examine the role of NS3 mutation identified on HCV RNA replication and on HCVtcp production, the N1586D mutation was introduced into pHH/SGR-Luc. Luciferase activities of the N1586D-mutated replicon were apparently lower than those of the WT-replicon, thus suggesting that the NS3 mutation reduced viral RNA replication (Fig. 7A). HCV RNA levels in the supernatants of cells transfected with WT- or mutant replicon plasmid along with pCAGC-NS2/JFH1am and luciferase activity in cells inoculated with supernatants from the transfected cells were then determined (Fig. 7B). The viral RNA level secreted from cells replicating the N1586D-mutated replicon was lower than that from cells replicating WT replicon (Fig. 7B, left). By contrast, a significantly higher infectivity of HCVtcp produced from the mutant replicon-cells was observed, as compared to WT replicon-cells (Fig. 7B, right), suggesting that the adaptive mutation increased the specific infectivity (almost 9-fold) of the virus particles. To further determine whether the N1586D mutation affects infectious viral assembly and/or virus release, we used the CD81-negative Huh-7 subclone, Huh7-25 (Akazawa et al., 2007), which may produce infectious particles, but is not susceptible to HCV entry due to a lack of CD81 expression, therefore allowing us to examine viral assembly and release without the influence of reinfection by produced HCVtcp. Measurement of intracellular and extracellular HCVtcp indicated that Huh7-25 cells replicating the N1586D-mutated replicon produced more infectious virus than WT in both supernatants and cell lysates (Fig. 7C). Thus, it can be concluded that the N1586D mutation contributes to enhanced infectious viral assembly, not RNA replication. We could not exclude the possibility that N1586D mutation affects virus release, since the mutation enhanced extracellular virus titers more than did the intracellular titer.

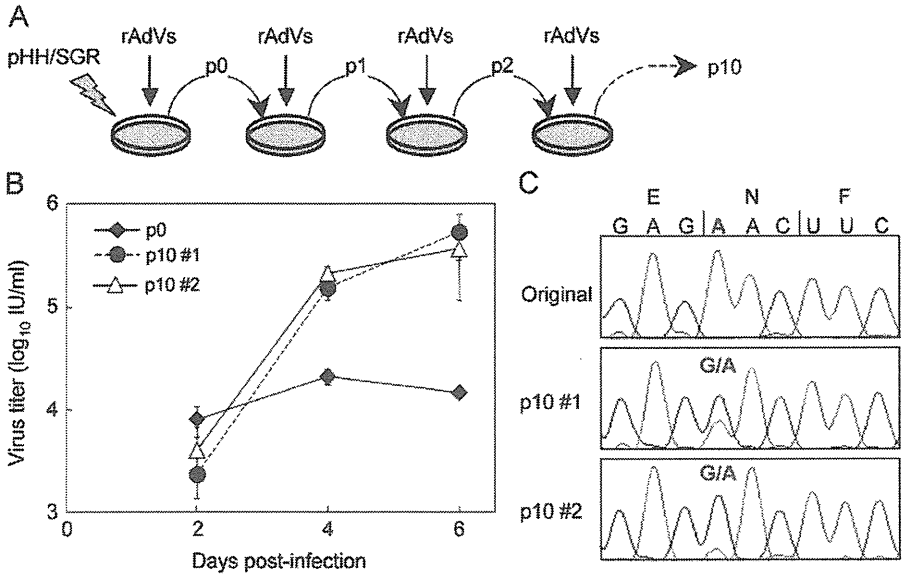

Fig. 6. Genotypic changes in HCVtcp following blind passage. (A) Experimental procedure for blind passage of HCVtcp. Huh7.5.1 cells were transfected with pHH/SGR and were doubly infected with AxCANCre and AxCALNLH-CNS2. Culture fluids were collected and were inoculated into cells infected with AxCANCre and AxCALNLH-CNS2. These procedures were repeated 10 times with two independent samples (#1 and #2). (B) Growth curves of HCVtcp p0 and p10 on Huh7.5.1 cells expressing core-NS2. Cells were infected with HCVtcp at an MOI of 0.05, and medium was collected at the indicated time points and subjected to titration. (C) Nucleotide sequences of original and blind-passaged replicons from HCVtcp. Nucleotides of mutated position are shown in red and bold.

The impact of the N1586D mutation on production of intra- and intergenotypic HCVtcp chimeras was also investigated. The N1586D mutation in the replicon enhanced the production of chimeric HCVtcp by providing core-p7 from all strains examined, although not statistically significant in THpa, and Con1 strains (Fig. 7D). Finally, to determine whether the N1586D mutation was responsible for enhancing HCVcc production, this mutation was introduced into pHHJFH1, which carries the full-length wild-type JFH-1 cDNA (Masaki et al., 2010), yielding pHHJFH1N1586D. The virus titer obtained from cells transfected with the pHHJFH1N1586D was significantly higher than that of WT (Fig. 7E), thus demonstrating that the N1586D mutation enhances yields of HCVcc, in addition to HCVtcp.

Discussion

Single-round infectious viral particles generated by *trans*-packaging systems are considered to be valuable tools for studying virus life cycles, particularly the steps related to entry into target cells, assembly and release of infectious particles. However, limited HCV strains have been applied for the efficient production of HCVtcp to date. In this study, we improved the HCVtcp system in order to enhance the productivity of infectious particles. Production of chimeric HCVtcp by providing genotype 1b-derived core-p7, in addition to intragenotypic viral proteins, was also confirmed. Furthermore, we exploited the system to investigate genetic changes during serial passage of target cells and identified a novel cell culture-adaptive mutation in NS3, which also contributes to enhance the productivity of HCVtcp.

HCVpp (Bartosch et al., 2003a; Hsu et al., 2003) has proven to be a valuable surrogate system by which the study of viral and cellular determinants of the viral entry pathway is possible. Early steps of HCV infection, including the role of HCV glycoprotein heterodimers, receptor binding, internalization and pH-dependent endosomal fusion, have been at least in part mimicked by HCVpp (Lavie et al., 2007). However, as HCVpp is generated in non-hepatic cells such as the human embryo kidney cells 293T, it is likely that the cell-derived component(s) of HCVpp differ from those of HCVcc. Hepatocytes play a role in maintaining lipid homeostasis in the body by assembling and secreting lipoproteins, including VLDL. It is highly likely that HCV exploits lipid synthesis pathways, as there is a tight link between virion formation and VLDL synthesis. Down-regulation of ApoE considerably reduces HCV production (Benga et al., 2010; Chang et al., 2007; Hishiki et al., 2010; Jiang and Luo, 2009; Owen et al., 2009). Infectivity of HCVcc is also neutralized by anti-ApoE antibodies (Chang et al., 2007). These data suggest that ApoE is important for HCV infectivity. Furthermore, Niemann-Pick C1-like 1 (NPC1L1), involving cholesterol uptake receptor, was recently identified as a host factor for HCV entry (Sainz et al., 2012). Knockdown of NPC1L1 had no effect on the entry of HCVpp whereas HCVcc entry was impaired, possibly due to different cholesterol content of these particles. Here, we found that the anti-ApoE antibody neutralized infection by HCVtcp and HCVcc, but not by HCVpp (Fig. 4A and C), thus suggesting that biogenesis and/or secretion pathways of VLDL are involved in HCVtcp similarly to HCVcc, but not in HCVpp.

We also observed that infectivity of HCVtcp and HCVcc is more efficiently neutralized by the anti-CD81 antibody, as compared to that of HCVpp (Fig. 4B and D). It has recently been reported that E2 of HCVcc contained both high-mannose-type and complex-type glycans, whereas most of the glycans on HCVpp-associated E2 were complex-type, which is matured by Golgi enzymes (Vieyres et al., 2010). Mutational analysis of the N-linked glycosylation sites in E1/E2 demonstrated that several glycans on E2 may affect the sensitivity of HCVpp against antibody neutralization, as well as access of CD81 to its binding site on E2 (Helle et al., 2010). The differences in sensitivity between HCVtcp and HCVpp to neutralization by anti-CD81 antibody observed here may be due to differences in carbohydrate composition of HCV glycoproteins during expression and processing of E1/E2 in cells and morphogenesis of HCVtcp and HCVpp.

By analyzing the various replicons for *trans*-packaging, we observed the highest production of HCVtcp with replicons from pHH/SGR, which lacked sequences not essential for RNA

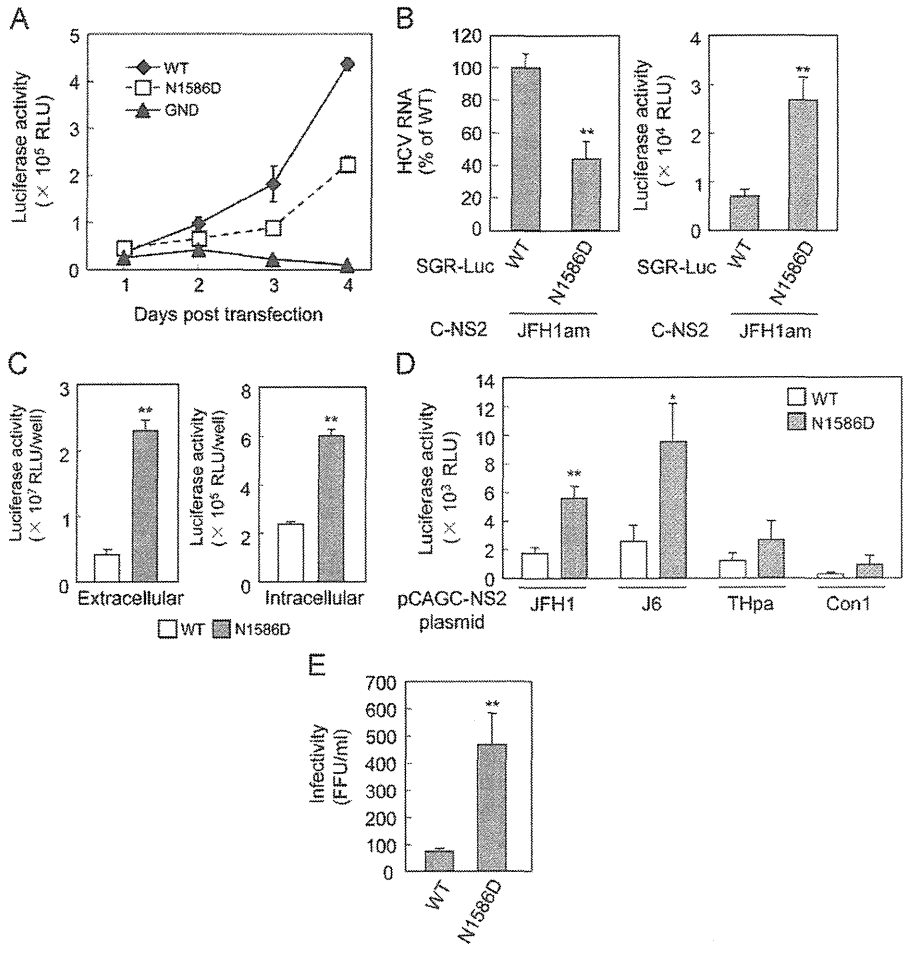

Fig. 7. Effects of N1586D mutation on RNA replication and production of HCVtcp or HCVcc. (A) RNA replication of replicons in cells transfected with pHH/SGR-Luc (WT) or N1586D mutant. Luciferase activities at 1 to 4 day post-transfection were determined. (B) Relative levels of HCV RNA in the supernatants from cells transfected with pHH/SGR-Luc (WT) or N1586D mutant plasmid along with pCAGC-NS2/JFH1am were shown in the left panel. Luciferase activities in cells inoculated with supernatants from cells transfected with indicated plasmids at 4 day post-transfection were shown in the right panel. (C) Luciferase activity in cells inoculated with supernatant and cell lysates from Huh7-25 cells transfected with pHH/SGR-Luc (WT) or N1586D mutant plasmid along with pCAGC-NS2/JFH1am at 5 day post-transfection. (D) Luciferase activity in cells inoculated with culture supernatant from cells transfected with pHH/SGR-Luc (WT) or N1586D mutant plasmid along with indicated core-NS2 plasmids at 4 day post-transfection. (E) Infectivity of supernatant from cells transfected with pHH/JFH1 (WT) or its derivative plasmid containing N1586D mutation at 6 day post-transfection. Statistical differences between WT and N1586D were evaluated using Student's *t*-test. $^{*}p < 0.05$, $^{**}p < 0.005$ vs. WT.

replication, while less efficient productivity was observed from pHH/SGR-Luc, pHH/SGR-C177, pHH/SGR-C191 and pHH/SGR-C-p7/am (Fig. 2C). Differences in the replication efficiency of the replicon do not appear to be a major determinant for HCVtcp productivity, at least in the present settings, as all replicon constructs except pHH/SGR-Luc replicated at similar levels, as confirmed by Western blotting (Fig. 2B). Although the shorter viral genome sequence may offer advantages over the longer sequence, further investigation is required in order to understand the molecular mechanisms underlying viral genome packaging. By comparing pHH/SGR vs. pHH/SGR-C177, pHH/SGR-C191 and pHH/SGR-C-p7/am, it is likely that the expression of the structural protein in *cis* does not increase HCVtcp production when sufficient amounts of structural proteins are supplied in *trans*.

Blind passage of HCVtcp in packaging cells infected with rAdVs providing core-NS2 enabled us to identify a novel culture-adaptive mutation in NS3. The N-terminal third of NS3 forms a serine protease, together with NS4A, and its C-terminal two-thirds exhibits RNA helicase and RNA-stimulated NTPase activities. In addition, similarly to flaviviruses (Kummerer and Rice, 2002; Liu et al., 2002), it is now apparent that HCV NS3 is also involved in viral morphogenesis (Han et al., 2009; Ma et al., 2008), although its precise role and underlying molecular mechanism(s) have not fully been elucidated. Two cell-culture adaptive NS3 mutations which are involved in HCV assembly have been identified. The Q1251L mutation in helicase subdomain 1 resulted in approximately 30-fold higher production of HCV without affecting NS3 enzymatic activities (Ma et al., 2008). The M1290K adaptive mutation was also located in subdomain 1 of the NS3 helicase (Han et al., 2009). The N1586D mutation identified here was located in subdomain 3 of helicase. Analogous to Q1251L and M1290K, the N1586D mutation enhanced the infectious viral assembly by increasing specific infectivity without affecting the efficiency of viral RNA replication. Considering the possibility that NS3 plays a role in linking between the viral replicase and assembly sites (Jones et al., 2011), it is likely that NS3 helicase is one of the determinants for interaction with the structural proteins. Our results, together with earlier studies, suggest that chimeric and defective mutations as well as supplying the viral components in *trans*, function as selective pressures in virion assembly.

In summary, we have established a plasmid-based reverse genetics for efficient production of HCVtcp with structural

proteins from various strains. Single-round infectious HCVtcp can complement the HCVcc and HCVpp systems as a valuable tool for the study of HCV life cycles.

Materials and methods

Cells

Huh7 derivative cell line Huh7.5.1 and Huh7-25 were maintained in Dulbecco modified Eagle medium (DMEM) supplemented with nonessential amino acids, 100 U of penicillin/mL, 100 μg of streptomycin/mL, and 10% fetal bovine serum at 37 °C in a 5% CO_2 incubator.

Plasmids

Plasmids pHHJFH1, pHH/SGR-Luc, pHH/SGR-Luc/GND and pCAG/C-NS2 were as described previously (Masaki et al., 2010). In this study, plasmid pCAG/C-NS2 was designated as pCAGC-NS2/JFH. The plasmid pCAGC-NS2/JFHam having adaptive mutations in E2 (N417S), p7 (N765D), and NS2 (Q1012R) in pCAGC-NS2/JFH was constructed by oligonucleotide-directed mutagenesis. These mutations were also introduced in pHHJFH1, resulting in pHHJFH1am. To generate core-NS2 expression plasmids with different strains of HCV, the cDNA coding core to the first transmembrane region of NS2 (33 amino acids) in pCAGC-NS2/JFH was replaced with the corresponding sequence of the J6 (Lindenbach et al., 2005), H77c (Yanagi et al., 1997), THpa (Shirakura et al., personal communication) and Con1 (Koch and Bartenschlager, 1999) strains. The THpa sequence contained the P to A mutation at 328 aa at E1 in the original TH strain. To generate pHH/SGR, pHH/SGR-Luc was digested with MluI and PmeI, followed by Klenow enzyme treatment and self-ligation to delete the luciferase coding sequence. To generate pHH/SGR-C177, pHH/SGR-C191 and pHH/SGR-C-p7/am, cDNA coding the partial core and luciferase in pHH/SGR-Luc were replaced with coding sequences for mature core (177aa), full-length core (191aa) or core-p7 polyprotein containing adaptive mutations in E2 and p7, respectively. The selected NS3 mutation (N1586D) was introduced into pHH/SGR-Luc and pHHJFH1 by oligonucleotide-directed mutagenesis.

Generation of viruses

HCVcc and HCVtcp were generated as described previously (Masaki et al., 2010). For the production of HCVpp-2a, plasmid pcDNAdeltaC-E1-E2(JFH1)am having adaptive mutations in E2 (N417S) in pcDNAdeltaC-E1-E2(JFH1) (Akazawa et al., 2007) was constructed by oligonucleotide-directed mutagenesis. Murine leukemia virus pseudotypes with VSV G glycoprotein expressing luciferase reporter (VSVpp) were generated in accordance with previously described methods (Akazawa et al., 2007; Bartosch et al., 2003a).

Luciferase assay

Huh7.5.1 cells were seeded onto a 24-well plate at a density of 3×10^4 cells/well 24 h prior to inoculation with reporter viruses. Cells were incubated for 72 h, followed by lysis with 100 μL of lysis buffer. Luciferase activity of the cells was determined using a luciferase assay system (Promega, Madison, WI). All luciferase assays were performed in triplicate.

Quantification of HCV infectivity and HCV RNA

To determine the titers of HCVtcp and HCVcc, Huh7.5.1 cell monolayers prepared in multi-well plates were incubated with dilutions of samples and then replaced with media containing 10% FBS and 0.8% carboxymethyl cellulose. Following incubation for 72 h, monolayers were fixed and immunostained with rabbit polyclonal anti-NS5A antibody, followed by Alexa Fluor 488-conjugated anti-rabbit secondary antibody (Invitrogen), and stained foci or individual cells were counted and used to calculate a titer of focus-forming units (FFU)/mL for spreading infections or infectious units (IU)/mL for non-spreading infections. For intracellular infectivity, the cell pellet was resuspended in culture media, and cells were lysed by four freeze–thaw cycles. Cell debris was pelleted by centrifugation for 5 min at 4000 rpm. Supernatant was collected and used for titration. To determine the amount of HCV RNA in culture supernatants, RNA was extracted from 140 μL of culture medium by QIAamp Viral RNA Mini Kit (QIAGEN, Valencia, CA) and treated with DNase (TURBO DNase; Ambion, Austin, TX) at 37 °C for 1 h. Extracted RNA was further purified by using an RNeasy Mini Kit, which includes RNase-free DNase digestion (QIAGEN). Copy numbers of HCV RNA were determined by real-time quantitative reverse transcription-PCR as described previously (Wakita et al., 2005).

Antibodies

Mouse monoclonal antibodies against actin (AC-15) and CD81 (JS-81) were obtained from Sigma (St. Louis, MO) and BD Biosciences (Franklin Lakes, NJ), respectively. Goat polyclonal antibody to ApoE (LV1479433) was obtained from Millipore (Tokyo, Japan). Anti-NS5A and anti-NS5B antibodies were rabbit polyclonal antibody against synthetic peptides.

Neutralization assay

For neutralization experiments with anti-CD81 antibody, Huh7.5.1 cells were incubated with dilutions of anti-CD81 antibody for 1 h at 37 °C. Cells were then infected with viruses for 5 h at 37 °C. For neutralization experiments with anti-ApoE antibody, viruses were incubated with various concentrations of anti-ApoE antibody at room temperature for 1 h and cells were infected with viruses for 5 h at 37 °C. Following infection, supernatant was removed and cells were incubated with culture medium, and luciferase activity was determined at 3 day post-infection for HCVtcp and pseudotyped viruses. For neutralization experiments with HCVcc generated with pHHJFH1am, a multiplicity of infection (MOI) of 0.05 was used for inoculation, and intracellular core protein levels were monitored by ELISA (Ortho Clinical Diagnostics) at 24 h post-infection.

Immunoblotting

Transfected cells were washed with PBS and incubated with lysis buffer (50 mM Tris–HCl, pH 7.4, 300 mM NaCl, 1% triton X-100). Lysates were then sonicated for 5 min and were added to the same volume of SDS sample buffer. Protein samples were boiled for 10 min, separated by SDS-PAGE, and transferred to PVDF membrane. After blocking, membranes were probed with first antibodies, followed by incubation with peroxidase-conjugated secondary antibody. Antigen–antibody complexes were visualized using an enhanced chemiluminescence detection system (Super Signal West Pico Chemiluminescent Substrate; PIERCE, Rockford, IL), in accordance with the manufacturer's protocols.

Generation of recombinant adenoviruses

rAdV, AxCANCre, expressing Cre recombinase tagged with nuclear localization signal under CAG promoter was prepared as described previously (Baba et al., 2005). The target rAdV AxCALNLH-CNS2 expressing HCV core-NS2 polyprotein with adaptive mutations in E2, p7 and NS2 was generated as follows. Cosmid pAxCALNLwit2 is identical to pAxCALNLw (Sato et al., 1998), except that both the terminal sequences of the rAdV genome are derived from pAxCAwit2 (Fukuda et al., 2006). The core-NS2 fragment obtained from pCAGC-NS2/JFH1am by StuI-EcoRI digestion and subsequent Klenow treatment was inserted into the SwaI site of pAxCALNLwit2. The resultant cosmid pAxCALNLH-CN2it2 was digested with PacI and transfected into 293 cells to generate rAdV AxCALNLH-CNS2.

Preparation of packaging cells for HCVtcp

Huh7.5.1 cells were coinfected with AxCANCre at an MOI of 1 and AxCALNLH-CNS2 at an MOI of 3 for expression of JFH-1 core-NS2 polyprotein containing the adaptive mutations in E2, p7 and NS2.

RNA preparation, RT-PCR and sequencing

Total cellular RNA was extracted with TRIzol reagent (Invitrogen, Carlsbad, CA), and subjected to reverse transcription with random hexamer and Superscript III reverse transcriptase (Invitrogen). Three fragments of HCV cDNAs that cover the entire HCV subgenomic replicon genome, were amplified by nested PCR with TaKaRa Ex Taq polymerase (Takara, Shiga, Japan). Amplified products were separated by agarose gel electrophoresis, and were used for direct DNA sequencing.

Acknowledgments

We are grateful to Francis V. Chisari (The Scripps Research Institute) for providing Huh7.5.1 cells. We thank M. Sasaki, M. Matsuda, and T. Date for their technical assistance, and T. Mizoguchi for the secretarial work. We also thank T. Masaki for their helpful discussions. This work was supported in part by grants-in-aid from the Ministry of Health, Labor, and Welfare and the Ministry of Education, Culture, Sports, Science, and Technology, Japan.

References

Adair, R., Patel, A.H., Corless, L., Griffin, S., Rowlands, D.J., McCormick, C.J., 2009. Expression of hepatitis C virus (HCV) structural proteins in trans facilitates encapsidation and transmission of HCV subgenomic RNA. J. Gen. Virol. 90 (Part 4), 833–842.

Akazawa, D., Date, T., Morikawa, K., Murayama, A., Miyamoto, M., Kaga, M., Barth, H., Baumert, T.F., Dubuisson, J., Wakita, T., 2007. CD81 expression is important for the permissiveness of Huh7 cell clones for heterogeneous hepatitis C virus infection. J. Virol. 81 (10), 5036–5045.

Baba, Y., Nakano, M., Yamada, Y., Saito, I., Kanegae, Y., 2005. Practical range of effective dose for Cre recombinase-expressing recombinant adenovirus without cell toxicity in mammalian cells. Microbiol. Immunol. 49 (6), 559–570.

Bartosch, B., Dubuisson, J., Cosset, F.L., 2003a. Infectious hepatitis C virus pseudoparticles containing functional E1-E2 envelope protein complexes. J. Exp. Med. 197 (5), 633–642.

Bartosch, B., Vitelli, A., Granier, C., Goujon, C., Dubuisson, J., Pascale, S., Scarselli, E., Cortese, R., Nicosia, A., Cosset, F.L., 2003b. Cell entry of hepatitis C virus requires a set of co-receptors that include the CD81 tetraspanin and the SR-B1 scavenger receptor. J. Biol. Chem. 278 (43), 41624–41630.

Benedicto, I., Molina-Jimenez, F., Bartosch, B., Cosset, F.L., Lavillette, D., Prieto, J., Moreno-Otero, R., Valenzuela-Fernandez, A., Aldabe, R., Lopez-Cabrera, M., Majano, P.L., 2009. The tight junction-associated protein occludin is required for a postbinding step in hepatitis C virus entry and infection. J. Virol. 83 (16), 8012–8020.

Benga, W.J., Krieger, S.E., Dimitrova, M., Zeisel, M.B., Parnot, M., Lupberger, J., Hildt, E., Luo, G., McLauchlan, J., Baumert, T.F., Schuster, C., 2010. Apolipoprotein E interacts with hepatitis C virus nonstructural protein 5A and determines assembly of infectious particles. Hepatology 51 (1), 43–53.

Chang, K.S., Jiang, J., Cai, Z., Luo, G., 2007. Human apolipoprotein E is required for infectivity and production of hepatitis C virus in cell culture. J. Virol. 81 (24), 13783–13793.

Cormier, E.G., Tsamis, F., Kajumo, F., Durso, R.J., Gardner, J.P., Dragic, T., 2004. CD81 is an entry coreceptor for hepatitis C virus. Proc. Natl. Acad. Sci. USA 101 (19), 7270–7274.

Evans, M.J., von Hahn, T., Tscherne, D.M., Syder, A.J., Panis, M., Wolk, B., Hatziioannou, T., McKeating, J.A., Bieniasz, P.D., Rice, C.M., 2007. Claudin-1 is a hepatitis C virus co-receptor required for a late step in entry. Nature 446 (7137), 801–805.

Flint, M., von Hahn, T., Zhang, J., Farquhar, M., Jones, C.T., Balfe, P., Rice, C.M., McKeating, J.A., 2006. Diverse CD81 proteins support hepatitis C virus infection. J. Virol. 80 (22), 11331–11342.

Fukuda, H., Terashima, M., Koshikawa, M., Kanegae, Y., Saito, I., 2006. Possible mechanism of adenovirus generation from a cloned viral genome tagged with nucleotides at its ends. Microbiol. Immunol. 50 (8), 643–654.

Han, Q., Xu, C., Wu, C., Zhu, W., Yang, R., Chen, X., 2009. Compensatory mutations in NS3 and NS5A proteins enhance the virus production capability of hepatitis C reporter virus. Virus Res. 145 (1), 63–73.

Helle, F., Vieyres, G., Elkrief, L., Popescu, C.I., Wychowski, C., Descamps, V., Castelain, S., Roingeard, P., Duverlie, G., Dubuisson, J., 2010. Role of N-linked glycans in the functions of hepatitis C virus envelope proteins incorporated into infectious virions. J. Virol. 84 (22), 11905–11915.

Hishiki, T., Shimizu, Y., Tobita, R., Sugiyama, K., Ogawa, K., Funami, K., Ohsaki, Y., Fujimoto, T., Takaku, H., Wakita, T., Baumert, T.F., Miyanari, Y., Shimotohno, K., 2010. Infectivity of hepatitis C virus is influenced by association with apolipoprotein E isoforms. J. Virol. 84 (22), 12048–12057.

Hoofnagle, J.H., 2002. Course and outcome of hepatitis C. Hepatology 36 (5 Suppl. 1), S21–9.

Hsu, M., Zhang, J., Flint, M., Logvinoff, C., Cheng-Mayer, C., Rice, C.M., McKeating, J.A., 2003. Hepatitis C virus glycoproteins mediate pH-dependent cell entry of pseudotyped retroviral particles. Proc. Natl. Acad. Sci. USA 100 (12), 7271–7276.

Ishii, K., Murakami, K., Hmwe, S.S., Zhang, B., Li, J., Shirakura, M., Morikawa, K., Suzuki, R., Miyamura, T., Wakita, T., Suzuki, T., 2008. Trans-encapsidation of hepatitis C virus subgenomic replicon RNA with viral structure proteins. Biochem. Biophys. Res. Commun. 371 (3), 446–450.

Jiang, J., Luo, G., 2009. Apolipoprotein E but not B is required for the formation of infectious hepatitis C virus particles. J. Virol. 83 (24), 12680–12691.

Jones, D.M., Atoom, A.M., Zhang, X., Kottilil, S., Russell, R.S., 2011. A genetic interaction between the core and NS3 proteins of hepatitis C virus is essential for production of infectious virus. J. Virol. 85 (23), 12351–12361.

Kanegae, Y., Lee, G., Sato, Y., Tanaka, M., Nakai, M., Sakaki, T., Sugano, S., Saito, I., 1995. Efficient gene activation in mammalian cells by using recombinant adenovirus expressing site-specific Cre recombinase. Nucl. Acids Res. 23 (19), 3816–3821.

Koch, J.O., Bartenschlager, R., 1999. Modulation of hepatitis C virus NS5A hyperphosphorylation by nonstructural proteins NS3, NS4A, and NS4B. J. Virol. 73 (9), 7138–7146.

Kummerer, B.M., Rice, C.M., 2002. Mutations in the yellow fever virus nonstructural protein NS2A selectively block production of infectious particles. J. Virol. 76 (10), 4773–4784.

Lavie, M., Goffard, A., Dubuisson, J., 2007. Assembly of a functional HCV glycoprotein heterodimer. Curr. Issues Mol. Biol. 9 (2), 71–86.

Lindenbach, B.D., Evans, M.J., Syder, A.J., Wolk, B., Tellinghuisen, T.L., Liu, C.C., Maruyama, T., Hynes, R.O., Burton, D.R., McKeating, J.A., Rice, C.M., 2005. Complete replication of hepatitis C virus in cell culture. Science 309 (5734), 623–626.

Liu, S., Yang, W., Shen, L., Turner, J.R., Coyne, C.B., Wang, T., 2009. Tight junction proteins claudin-1 and occludin control hepatitis C virus entry and are downregulated during infection to prevent superinfection. J. Virol. 83 (4), 2011–2014.

Liu, W.J., Sedlak, P.L., Kondratieva, N., Khromykh, A.A., 2002. Complementation analysis of the flavivirus Kunjin NS3 and NS5 proteins defines the minimal regions essential for formation of a replication complex and shows a requirement of NS3 in cis for virus assembly. J. Virol. 76 (21), 10766–10775.

Ma, Y., Yates, J., Liang, Y., Lemon, S.M., Yi, M., 2008. NS3 helicase domains involved in infectious intracellular hepatitis C virus particle assembly. J. Virol. 82 (15), 7624–7639.

Masaki, T., Suzuki, R., Saeed, M., Mori, K., Matsuda, M., Aizaki, H., Ishii, K., Maki, N., Miyamura, T., Matsuura, Y., Wakita, T., Suzuki, T., 2010. Production of infectious hepatitis C virus by using RNA polymerase I-mediated transcription. J. Virol. 84 (11), 5824–5835.

Mazumdar, B., Banerjee, A., Meyer, K., Ray, R., 2011. Hepatitis C virus E1 envelope glycoprotein interacts with apolipoproteins in facilitating entry into hepatocytes. Hepatology 54 (4), 1149–1156.

McKeating, J.A., Zhang, L.Q., Logvinoff, C., Flint, M., Zhang, J., Yu, J., Butera, D., Ho, D.D., Dustin, L.B., Rice, C.M., Balfe, P., 2004. Diverse hepatitis C virus glycoproteins mediate viral infection in a CD81-dependent manner. J. Virol. 78 (16), 8496–8505.

Owen, D.M., Huang, H., Ye, J., Gale Jr., M., 2009. Apolipoprotein E on hepatitis C virion facilitates infection through interaction with low-density lipoprotein receptor. Virology 394 (1), 99–108.

Pietschmann, T., Kaul, A., Koutsoudakis, G., Shavinskaya, A., Kallis, S., Steinmann, E., Abid, K., Negro, F., Dreux, M., Cosset, F.L., Bartenschlager, R., 2006. Construction and characterization of infectious intragenotypic and intergenotypic hepatitis C virus chimeras. Proc. Natl. Acad. Sci. USA 103 (19), 7408–7413.

Pileri, P., Uematsu, Y., Campagnoli, S., Galli, G., Falugi, F., Petracca, R., Weiner, A.J., Houghton, M., Rosa, D., Grandi, G., Abrignani, S., 1998. Binding of hepatitis C virus to CD81. Science 282 (5390), 938–941.

Ploss, A., Evans, M.J., Gaysinskaya, V.A., Panis, M., You, H., de Jong, Y.P., Rice, C.M., 2009. Human occludin is a hepatitis C virus entry factor required for infection of mouse cells. Nature 457 (7231), 882–886.

Russell, R.S., Meunier, J.C., Takikawa, S., Faulk, K., Engle, R.E., Bukh, J., Purcell, R.H., Emerson, S.U., 2008. Advantages of a single-cycle production assay to study cell culture-adaptive mutations of hepatitis C virus. Proc. Natl. Acad. Sci. USA 105 (11), 4370–4375.

Sainz Jr., B., Barretto, N., Martin, D.N., Hiraga, N., Imamura, M., Hussain, S., Marsh, K.A., Yu, X., Chayama, K., Alrefai, W.A., Uprichard, S.L., 2012. Identification of the Niemann-Pick C1-like 1 cholesterol absorption receptor as a new hepatitis C virus entry factor. Nat. Med. 18 (2), 281–285.

Sato, Y., Tanaka, K., Lee, G., Kanegae, Y., Sakai, Y., Kaneko, S., Nakabayashi, H., Tamaoki, T., Saito, I., 1998. Enhanced and specific gene expression via tissue-specific production of Cre recombinase using adenovirus vector. Biochem. Biophys. Res. Commun. 244 (2), 455–462.

Scarselli, E., Ansuini, H., Cerino, R., Roccasecca, R.M., Acali, S., Filocamo, G., Traboni, C., Nicosia, A., Cortese, R., Vitelli, A., 2002. The human scavenger receptor class B type I is a novel candidate receptor for the hepatitis C virus. EMBO J. 21 (19), 5017–5025.

Steinmann, E., Brohm, C., Kallis, S., Bartenschlager, R., Pietschmann, T., 2008. Efficient trans-encapsidation of hepatitis C virus RNAs into infectious virus-like particles. J. Virol. 82 (14), 7034–7046.

Suzuki, T., Ishii, K., Aizaki, H., Wakita, T., 2007. Hepatitis C viral life cycle. Adv. Drug Deliv. Rev. 59 (12), 1200–1212.

Tani, H., Komoda, Y., Matsuo, E., Suzuki, K., Hamamoto, I., Yamashita, T., Moriishi, K., Fujiyama, K., Kanto, T., Hayashi, N., Owsianka, A., Patel, A.H., Whitt, M.A., Matsuura, Y., 2007. Replication-competent recombinant vesicular stomatitis virus encoding hepatitis C virus envelope proteins. J. Virol. 81 (16), 8601–8612.

Vieyres, G., Thomas, X., Descamps, V., Duverlie, G., Patel, A.H., Dubuisson, J., 2010. Characterization of the envelope glycoproteins associated with infectious hepatitis C virus. J. Virol. 84 (19), 10159–10168.

Wakita, T., Pietschmann, T., Kato, T., Date, T., Miyamoto, M., Zhao, Z., Murthy, K., Habermann, A., Krausslich, H.G., Mizokami, M., Bartenschlager, R., Liang, T.J., 2005. Production of infectious hepatitis C virus in tissue culture from a cloned viral genome. Nat. Med. 11 (7), 791–796.

Yanagi, M., Purcell, R.H., Emerson, S.U., Bukh, J., 1997. Transcripts from a single full-length cDNA clone of hepatitis C virus are infectious when directly transfected into the liver of a chimpanzee. Proc. Natl. Acad. Sci. USA 94 (16), 8738–8743.

Zhong, J., Gastaminza, P., Cheng, G., Kapadia, S., Kato, T., Burton, D.R., Wieland, S.F., Uprichard, S.L., Wakita, T., Chisari, F.V., 2005. Robust hepatitis C virus infection in vitro. Proc. Natl. Acad. Sci. USA 102 (26), 9294–9299.

JCM
Journals.ASM.org

Japanese Reference Panel of Blood Specimens for Evaluation of Hepatitis C Virus RNA and Core Antigen Quantitative Assays

Asako Murayama,[a] Nao Sugiyama,[a] Koichi Watashi,[a] Takahiro Masaki,[a] Ryosuke Suzuki,[a] Hideki Aizaki,[a] Toshiaki Mizuochi,[b] Takaji Wakita,[a] and Takanobu Kato[a]

Department of Virology II, National Institute of Infectious Diseases, Tokyo, Japan,[a] and Department of Research on Blood and Biological Products, National Institute of Infectious Diseases, Tokyo, Japan[b]

An accurate and reliable quantitative assay for hepatitis C virus (HCV) is essential for measuring viral propagation and the efficacy of antiviral therapy. There is a growing need for domestic reference panels for evaluation of clinical assay kits because the performance of these kits may vary with region-specific genotypes or polymorphisms. In this study, we established a reference panel by selecting 80 donated blood specimens in Japan that tested positive for HCV. Using this panel, we quantified HCV viral loads using two HCV RNA kits and five core antigen (Ag) kits currently available in Japan. The data from the two HCV RNA assay kits showed excellent correlation. All RNA titers were distributed evenly across a range from 3 to 7 log IU/ml. Although the data from the five core Ag kits also correlated with RNA titers, the sensitivities of individual kits were not sufficient to quantify viral load in all samples. As calculated by the correlation with RNA titers, the theoretical lower limits of detection by these core Ag assays were higher than those for the detection of RNA. Moreover, in several samples in our panel, core Ag levels were underestimated compared to RNA titers. Sequence analysis in the HCV core region suggested that polymorphisms at amino acids 47 to 49 of the core Ag were responsible for this underestimation. The panel established in this study will be useful for estimating the quality of currently available and upcoming HCV assay kits; such quality control is essential for clinical usage of these kits.

Hepatitis C virus (HCV) is a major cause of chronic liver disease worldwide (15). There is no protective vaccine against this virus, and once an individual is infected, HCV often establishes persistent infection and leads to chronic hepatitis, cirrhosis, and hepatocellular carcinoma (9). The most widely used therapy for HCV infection is the combined administration of pegylated alpha interferon and ribavirin (29). However, this treatment is problematic, as it has limited efficacy, high cost, and severe adverse effects (8, 25). To estimate the outcome of antiviral therapy, and to understand the state of viral propagation, it is important to determine the HCV viral load in chronic hepatitis C patients by the use of accurate and reliable HCV quantitative assays (9, 14). For this purpose, several commercial assay kits for HCV RNA and core antigen (Ag) quantification are currently used in Japan. For quantification of HCV RNA levels, two real-time quantitative reverse transcription-PCR (qRT-PCR)-based assay kits are available, including the COBAS AmpliPrep/COBAS TaqMan HCV test (CAP/CTM-RNA; Roche Diagnostics, Tokyo, Japan) and the Abbott RealTime HCV test (ART-RNA; Abbott Japan, Tokyo, Japan). These assays are known to have high sensitivity and a wide dynamic range, but they require technical skill and attention to maintaining the specified conditions (4–6, 16, 24, 33–35). Alternatively, HCV viremia can be quantified by assessment of HCV core Ag level (1–3, 7, 10, 12, 13, 17–22, 27, 30–32). Five HCV core Ag assay kits are commercially available in Japan, including Architect HCV Ag (Architect-Ag; Abbott Japan), Lumipulse Ortho HCV Ag (Lumipulse-Ag; Fujirebio, Tokyo, Japan), Lumispot Eiken HCV Ag (Lumispot-Ag; Eiken Chemical, Tokyo, Japan), the Ortho HCV Ag ELISA test (ELISA-Ag; Ortho Clinical Diagnostics, Tokyo, Japan), and the Ortho HCV Ag IRMA test (IRMA-Ag; Ortho Clinical Diagnostics, Tokyo, Japan). These assays have some disadvantages compared to those measuring HCV RNA (notably, low sensitivity and narrow range of quantification) but also have some advantages (including ease of use, reduced risk of contamination, reduced cost, and reliability even with samples stored at room temperature for extended periods of time [1, 32]). Although core Ag levels are thought to be related closely to HCV RNA titers, the correlation and linearity of core Ag levels have not yet been fully evaluated. In addition, these quantitative parameters are known to be affected by nucleotide and amino acid sequences at the target regions of the assays (5, 6, 28, 34), and this sequence variation depends on genotypes or predominant strains in specific geographical regions.

In this study, we established a Japanese reference panel of samples for evaluation of HCV RNA and core Ag levels by collecting donated blood specimens that tested positive for HCV RNA and anti-HCV antibodies. Using this reference panel, we evaluated the HCV loads in these specimens with two HCV RNA assay kits and five core Ag assay kits and assessed correlations among the data generated by these kits.

MATERIALS AND METHODS

Preparation of reference panel. To establish a reference panel for HCV quantitative assays, a total of 80 donated plasma samples were selected. All of these specimens, supplied by the Japanese Red Cross Blood Centers, tested positive for the presence of HCV RNA and anti-HCV antibodies. These samples, collected in Japan from May to September of 2007, were obtained from Japanese blood donor volunteers in various regions of

Received 20 February 2012 Returned for modification 21 March 2012
Accepted 30 March 2012
Published ahead of print 11 April 2012
Address correspondence to Takanobu Kato, takato@nih.go.jp.
Supplemental material for this article may be found at http://jcm.asm.org/.

doi:10.1128/JCM.00487-12

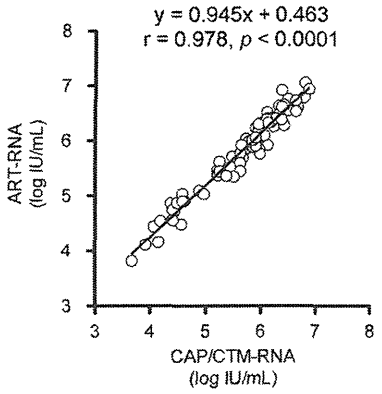

FIG 1 Correlation of HCV RNA titers as quantified by two commercial kits.

Japan. The samples were divided into 1-ml aliquots and stored at −80°C until use.

Quantification of HCV RNA and core Ag. The HCV RNA titer was measured with two real-time qRT-PCR kits, CAP/CTM-RNA (detection range, 1.5×10^1 to 6.9×10^7 IU/ml) and ART-RNA (detection range, 1.2×10^1 to 1.0×10^8 IU/ml). Additionally, samples were assessed using five HCV core Ag assay kits, including Architect-Ag (detection range, 3 to 20,000 fmol/liter), Lumipulse-Ag (detection range, 50 to 50,000 fmol/liter), Lumispot-Ag (detection range, 20 to 400,000 fmol/liter), ELISA-Ag (detection range, 44.4 to 3,600 fmol/liter), and IRMA-Ag (detection range, 20 to 20,000 fmol/liter). All assays were performed by the respective manufacturers at their research laboratories.

Sequencing and genotyping of HCV in reference panel samples. Viral RNA was extracted with the QIAamp viral RNA kit (Qiagen, Valencia, CA) from 140 μl of each plasma sample. HCV RNA was amplified by RT-PCR with primers corresponding to the 5′ untranslated region (UTR) (43S-IH, 5′-CCTGTGAGGAACTACTGTCTTC-3′; c/s17-ssp, 5′-CCGGGAGAGCCATAGTGGTCTGCG-3′) and the E1 region (1323R-IH, 5′-GGCGACCAGTTCATCATCAT-3′); the amplified products were sequenced directly. HCV genotypes of the isolated strains were assigned by phylogenetic analysis using an alignment with a representative strain of each genotype.

Statistical analysis. The correlations of obtained quantitative data were assessed by Pearson's correlation coefficient analysis, and values for r and P were calculated. A P value of <0.05 was considered to indicate statistical significance. Analysis was performed using Prism 5 software (GraphPad Software, Inc., La Jolla, CA).

Nucleotide sequence accession numbers. The accession numbers of C-01 to C-80 are AB705312 to AB705391, respectively.

RESULTS

Quantification of HCV RNA levels. The reference panel established in this work was used to measure HCV RNA levels with the CAP/CTM-RNA and ART-RNA kits. The correlation of the data obtained with the two kits is shown in Fig. 1. The RNA titers of these samples were distributed evenly, and all values were within the dynamic ranges of both assays. The HCV titers ranged from 3.68 to 6.88 and 3.82 to 7.08 log IU/ml in CAP/CTM-RNA and ART-RNA, respectively, and the correlation was significant ($r = 0.978$; $P < 0.0001$).

Quantification of HCV core Ag levels. HCV core Ag levels were measured using Architect-Ag, Lumipulse-Ag, Lumispot-Ag, ELISA-Ag, and IRMA-Ag kits. Among the 80 specimens in the reference panel, core Ag levels could be measured in all samples using Architect-Ag and ELISA-Ag kits, whereas core Ag levels were below the detection limit in 4, 2, and 1 samples using Lumipulse-Ag, Lumispot-Ag, and IRMA-Ag kits, respectively (Fig. 2; also, see Fig. S1 in the supplemental material). Significant correlations were observed between assays of HCV core Ag and HCV RNA ($r = 0.9065$ to 0.9666 and $P < 0.0001$ compared with CAP/CTM-RNA data [Fig. 2]); $r = 0.8877$ to 0.9552 and $P < 0.0001$ compared with ART-RNA data [see Fig. S1 in the supplemental material]). The theoretical lower limits of detection of these assays were calculated by use of these correlation formulas and were 3.2 and 3.4 log IU/ml for Architect-Ag, 4.2 and 4.2 log IU/ml for Lumipulse-Ag, 3.7 and 3.9 log IU/ml for Lumispot-Ag, 3.6 and 3.8 log IU/ml for ELISA-Ag, and 3.6 and 3.8 log IU/ml for IRMA-Ag (compared to CAP/CTM-RNA and ART-RNA, respectively). These calculated detection limits were substantially higher than those for the RNA quantitative assays (1.18 and 1.08 log IU/ml for CAP/CTM-RNA and ART-RNA, respectively).

In addition, we found that several samples showed considerable deviation from the linear regression (Fig. 2; also, see Fig. S1 in the supplemental material). To identify the deviating samples, we used Bland-Altman plot analysis (Fig. 3; also, see Fig. S2 in the supplemental material). This plot shows the difference between the titer values of HCV RNA and core Ag as a function of the average of these two values. Several samples demonstrated discordance between the measured HCV RNA and core Ag levels. Among these samples, we focused on samples with discordant results in multiple core Ag assays compared to both RNA quantitative assays. For sample C-01, core Ag levels were underestimated when measured with Architect-Ag, Lumipulse-Ag, and Lumispot-Ag in comparison with CAP/CTM-RNA (Fig. 3) and when measured with Architect-Ag, Lumipulse-Ag, Lumispot-Ag, and IRMA-Ag in comparison with ART-RNA (see Fig. S2 in the supplemental material). Likewise, for sample C-73, core Ag levels were underestimated when measured with Architect-Ag, Lumipulse-Ag, and IRMA-Ag in comparison with CAP/CTM-RNA (Fig. 3) and when measured with Architect-Ag and Lumipulse-Ag in comparison with ART-RNA (see Fig. S2 in the supplemental material). Thus, sample-specific underestimation was observed in several HCV core Ag kits.

Nucleotide sequences in core region of reference panel samples. To clarify the sources of these underestimates of HCV core Ag levels, HCV RNA was extracted from each of the samples in the reference panel, and the nucleotide sequences of core regions were determined. Phylogenetic analysis with these sequences permitted classification of the individual strains by genotype. Of 80 samples in the reference panel, 1 (1.3%) was genotype 1a, 35 (43.8%) were genotype 1b, 26 (32.5%) were genotype 2a, and 18 (22.5%) were genotype 2b (Table 1; also, see Fig. S3 in the supplemental material). These strains were distributed evenly among reference strains of each genotype and cover the sequence diversity of strains isolated in Japan (see Fig. S3 in the supplemental material). The genotypes of samples associated with underestimated core Ag values (samples C-01 and C-73) were both classified as genotype 2a.

Predicted amino acid sequences of HCV core protein were aligned with the consensus core protein sequence for the genotype 1b strains obtained in this study (see Fig. S4 in the supplemental material). Excluding the genotype-specific sequence variations, a specific amino acid polymorphism was identified at amino acid (aa) residue 48 (Ala to Thr) in samples C-01 and C-73. Sample C-01, which yielded underestimated values in most core Ag assays, also possessed an additional polymorphism in the same region,

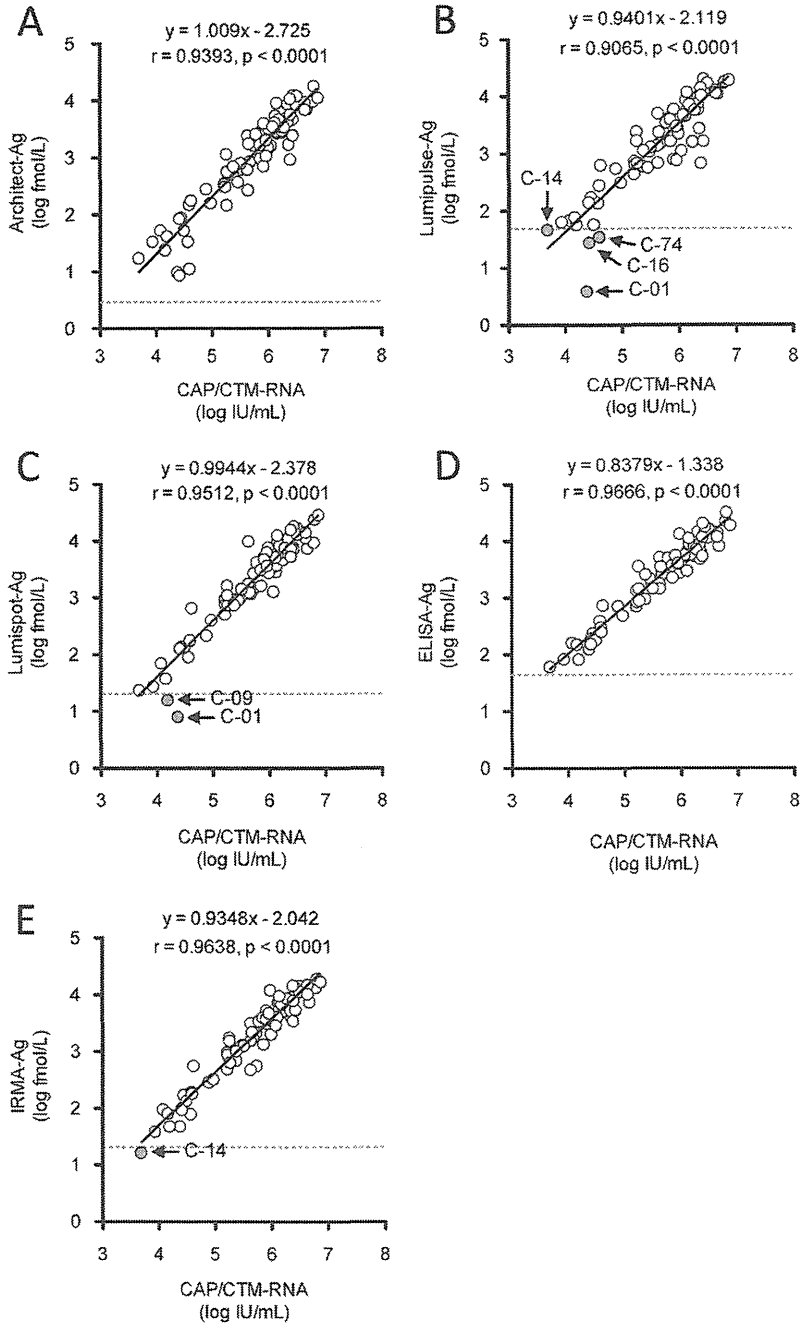

FIG 2 Correlation between CAP/CTM-RNA and core Ag levels as quantified by five commercial kits. Data for core Ag levels were converted to log fmol/liter prior to analysis. In each plot, the lower limit of detection of the respective core Ag assay is indicated by a dotted line. Data for samples below the lower detection limit of each assay are indicated by shaded circles labeled with the respective sample designations.

specifically an Arg-to-Gly substitution at aa 47. We suspected that these polymorphisms altered the antigenicity of the core protein, thereby reducing detected core Ag levels and leading to underestimation of values by the core Ag quantification kits. To assess the correlation of these polymorphisms with the underestimation of core Ag values, strains containing polymorphisms in this region (at aa 47 to 49 [Fig. 4]) were identified in Bland-Altman plots of HCV RNA and core Ag (Fig. 3; also, see Fig. S2 in the supplemental material). A total of 12 strains exhibited polymorphisms at these positions, including 2 strains of genotype 1b, 8 of genotype 2a, and 2 of genotype 2b (Table 1). In the Bland-Altman plot of CAP/CTM-RNA and Architect-Ag, 4 of 12 values (for samples C-01, C-16, C-73, and C-74) were located under the line of the lower 95% limit of agreement (Fig. 3A). Likewise, in the plot of CAP/CTM-RNA and Lumipulse-Ag, 3 of 12 values (those for samples C-01, C-67, and C-73) were located under the line of the lower

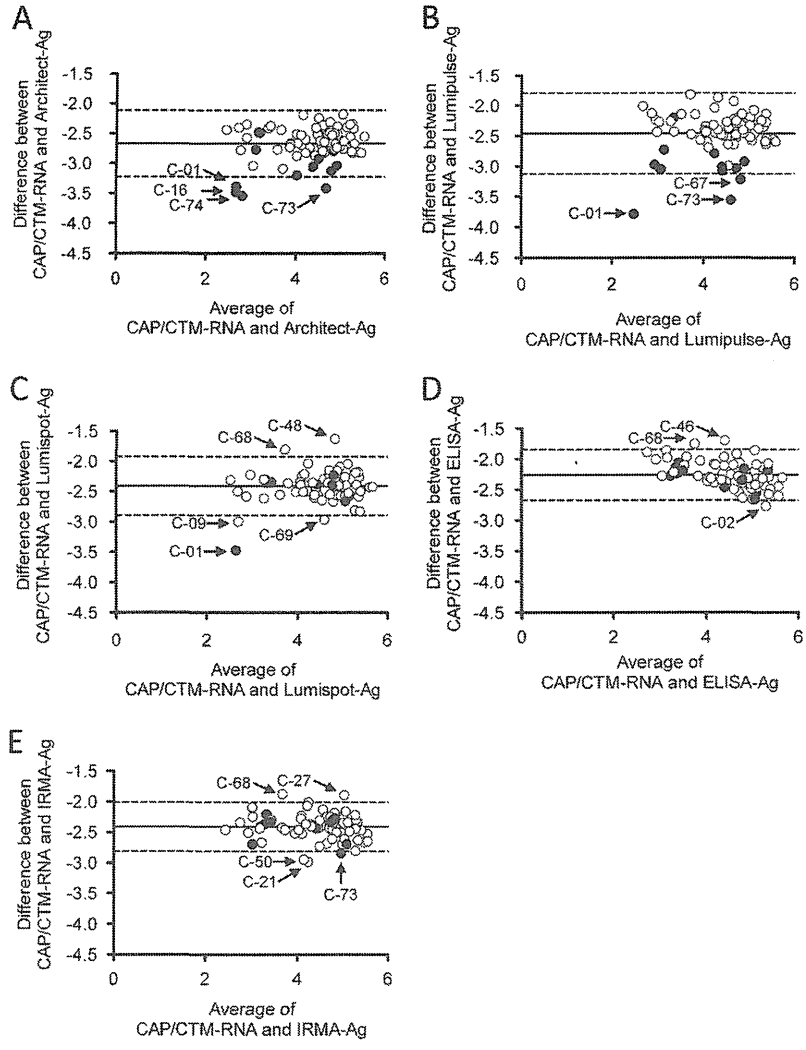

FIG 3 Bland-Altman plot analysis of CAP/CTM-RNA and core Ag levels as quantified by five commercial kits. These plots show the difference between the values of HCV RNA and core Ag as a function of the average of these two values. Data for core Ag levels were converted to log fmol/liter prior to analysis. The bias and 95% limits of agreements are indicated by solid and dashed lines, respectively. Data for samples with polymorphisms at amino acid residues 47 to 49 are indicated by solid circles. Data points outside the 95% limits are indicated by arrows labeled with the sample designations.

95% limit of agreement (Fig. 3B). In these plots, underestimation for samples that lacked these polymorphisms (at aa 47 to 49) was not detected. In the plot of CAP/CTM-RNA and Lumispot-Ag, only 1 sample (C-01) was located under the line of the lower 95% limit of agreement, but this sample exhibited the most discordant value (Fig. 3C). In the plot of CAP/CTM-RNA and ELISA-Ag, no correlation between polymorphisms at these positions and underestimation was observed (Fig. 3D). In the plot of CAP/CTM-RNA and IRMA-Ag, sample C-73 was located under the line of the lower 95% limit of agreement, as were other samples that lacked polymorphisms at aa 47 to 49 (Fig. 3E). Similar trends were observed in comparison with ART-RNA levels (see Fig. S2 in the supplemental material). Based on these results, the levels of HCV core Ag measured with Architect-Ag and Lumipulse-Ag seem to be more strongly affected by single polymorphisms at these positions. In the case of Lumispot-Ag, underestimation may be limited to specimens with multiple polymorphisms at these positions.

TABLE 1 Number of reference panel strains with polymorphisms at amino acid residues 47 to 49 of the HCV core region

Genotype	No. (%) of strains	
	Total	With polymorphisms
1a	1	0
1b	35	2 (5.7)
2a	26	8 (30.8)
2b	18	2 (11.8)
Total	80	12 (15.0)

DISCUSSION

The quantification of HCV viral load is essential for selecting an appropriate antiviral strategy and for monitoring the efficacy of treatment. Since HCV is known to be highly variable and rapidly

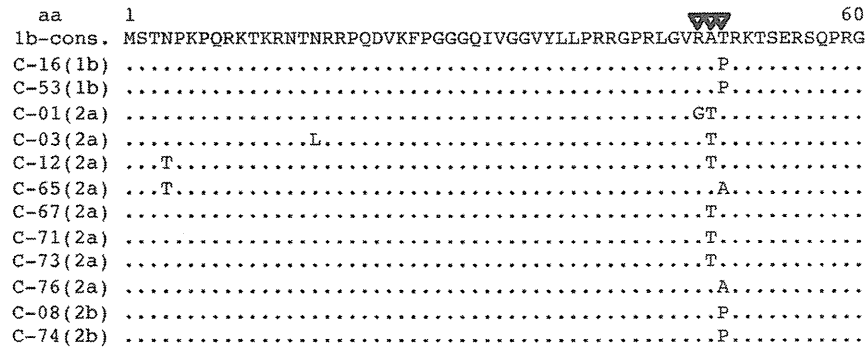

FIG 4 Alignment of the first 60 amino acids of the HCV core region of strains with polymorphisms at amino acid residues 47 to 49. The position numbers are given at the top. Dots indicate identical amino acids. The consensus sequence of 1b strains (1b cons.) isolated in this study was determined and used as a reference sequence. Genotypes of strains are given in parentheses. Positions of polymorphisms are indicated by inverted triangles above the sequence alignment.

evolving (23, 26), the assays for quantifying this virus should be unaffected by sequence polymorphisms. In this study, we established a reference panel with HCV-positive samples and evaluated the correlation among multiple assays for HCV RNA and core Ag quantification.

Using this reference panel, we found that the results from two HCV RNA assay kits, CAP/CTM-RNA and ART-RNA, correlated with excellent agreement ($r = 0.978$, $P < 0.0001$ [Fig. 1]), although discrepancies for values generated by these two assays have been reported for strains of genotypes 1, 2, and 4 (5, 6, 34). In Japan, the prevalent genotypes are 1b, 2a, and 2b (11); no genotype 4 sample was included in our reference panel (Table 1). In quantification with CAP/CTM-RNA, underestimation of HCV RNA titer has been reported for French genotype 2 samples (5). In our panel, no underestimation was observed for data from genotype 2 samples compared to values obtained using ART-RNA. Therefore, underestimation in quantification with CAP/CTM-RNA is expected to be rare in Japanese samples, and the two assays for HCV RNA quantification should be considered accurate and reliable, at least for Japanese samples. Additionally, the prepared reference panel appears to be suitable for the evaluation of HCV quantification assays, because genotypes of samples in this panel are representative of those found in Japan and viral loads are distributed evenly across the range of expected titers.

The quantification of HCV core Ag is an alternative test for HCV infection and viral load. However, in this study, several core Ag quantitative assays failed to provide accurate results for all of the samples in the reference panel (Fig. 2). Some quantified values were below the kits' detection limits. This shortcoming was mainly attributable to the lower sensitivity of the core Ag assay kits; increased sensitivity is urged in the future development of HCV core Ag kits. Among the kits tested here, Architect-Ag assay exhibited the highest sensitivity and was sufficient for quantifying the viral load in all samples. However, even in the case of Architect-Ag, theoretical lower limits of detection, calculated by correlation formula using CAP/CTM-RNA and ART-RNA, were 3.2 and 3.4 log IU/ml, respectively; these detection limits still exceeded the lower limits of the HCV RNA quantification assays. Therefore, the sensitivity of the available HCV core Ag assays is still insufficient to detect low-titer HCV infections. Core Ag kits therefore may be unsuitable for the detection of breakthrough hepatitis during antiviral therapy or for the detection of HCV infection in a window period.

Comparison between HCV RNA and core Ag assays revealed good correlations, with r coefficients ranging from 0.8877 to 0.9666 and P values being less than 0.0001 (Fig. 2; also, see Fig. S1 in the supplemental material). Therefore, the HCV core Ag levels may serve as an alternative to HCV RNA levels when titers remain within the detection ranges of the core Ag kits. However, several discordances were detected when core Ag levels were compared with those of HCV RNA. For one sample in our panel (sample C-01), core Ag levels were lower than expected when quantified using any of the three core Ag kits (Architect-Ag, Lumipulse-Ag, and Lumispot-Ag) (Fig. 3; also, see Fig. S2 in the supplemental material). Another sample (C-73) also yielded lower-than-expected levels when assayed with Architect-Ag and Lumipulse-Ag kits. Sequence analysis of the core region revealed that polymorphisms at aa 47 and 48 correlated with these underestimates by core Ag kits (see Fig. S4 in the supplemental material). These results are consistent with our previous study, which suggested that core Ag levels of HCV strain JFH-1 were underestimated by the Lumipulse-Ag kit in comparison to the ELISA-Ag assay (28). Strain JFH-1 harbors an Ala-to-Thr substitution at aa 48; conversion of Thr to Ala at this position in JFH-1 was sufficient to overcome this underestimation. This region of the core Ag presumably corresponds to one of the epitopes recognized by the monoclonal antibodies used in the Lumipulse-Ag kit, such that polymorphisms at this position affected the antigenicity of the core protein. In this study, we found that the presence of other polymorphisms in this region (aa 47 to 49) correlated with reduced core Ag levels as detected by Lumipulse-Ag, as well as by other assays (Architect-Ag and Lumispot-Ag). Sample C-01 demonstrated a drastic deviation from expected core Ag levels in these assays (Fig. 3; also, see Fig. S2 in the supplemental material). The HCV strain in this sample contains two polymorphisms (Arg to Gly at aa 47 and Ala to Thr at aa 48); the multiple polymorphisms may impair antibody binding more severely and therefore result in underestimation of core Ag levels. Interestingly, this sample exhibited reasonable core Ag levels when assayed using ELISA-Ag. Thus, the underestimation of core protein levels in this sample was kit dependent, suggesting the targeting of distinct epitopes by the antibodies used in each of these kits. This hypothesis could not be confirmed, because the identity of the epitopes targeted by each kit is proprietary.

Of 12 samples with amino acid polymorphisms in this region, 2 (5.7%) were of genotype 1b, 8 (30.8%) were of genotype 2a, and

TABLE 2 Number of strains in the sequence database[a] with polymorphisms at amino acid residues 47 to 49 of the HCV core region

Genotype	No. (%) of strains				
		With polymorphism			
	Tested	At aa 47 (R/C, G)	At aa 48 (A/T, P)	At aa 49 (T/A, P, L)	Total
1b	543	2 (0.36)	4 (0.74)	16 (2.96)	22 (4.1)
2a	24	0	6 (25.0)	1 (4.2)	7 (29.2)
2b	39	0	0	2 (6.9)	2 (6.9)

[a] http://s2as02.genes.nig.ac.jp/.

2 (11.8%) were of genotype 2b (Table 1). Searches of the Hepatitis Virus Database (http://s2as02.genes.nig.ac.jp/) revealed that corresponding amino acid polymorphisms were observed in 22 of 543 strains (4.1%) of genotype 1b, 7 of 24 strains (29.2%) of genotype 2a, and 2 of 39 strains (6.9%) of genotype 2b (Table 2). These percentages were consistent with our observations in the proposed reference panel. These data (our results and those from the database) clearly indicate that genotype 2a strains are the most frequent source of underestimation of core Ag levels. Notably, our search of the sequence database did not yield any HCV strain with multiple polymorphisms in the region from aa 47 to 49, as we saw in our sample C-01. Therefore, strains with such multiple polymorphisms are rare so far, but detection of this isolate among donated blood specimens suggests that such HCV strains could be emerging in clinical samples. For patients harboring such strains, HCV viral load may be underestimated if measurement of HCV viral load is performed by core Ag assay. Such underestimates may result in erroneous selection of therapy, adversely affecting patient outcome. Thus, this shortcoming in HCV core Ag assay kits needs to be addressed.

There is a growing need for evaluation of clinical assay kits with domestic specimen reference panels, since the performance of these kits may be affected by the genotypes or polymorphisms of predominant strains in different geographic regions. To our knowledge, such an investigation of HCV clinical assay kits with domestic specimens has not previously been conducted in Japan. The Japanese HCV reference panel described here was generated with plasma samples collected from Japanese volunteers. Each sample was divided into small aliquots, and the panel was prepared in multiple sets. The samples in our HCV reference panel represent the predominant strains and genotypes seen in Japan. We expect that this reference panel will be of use for the development, evaluation, and optimization of HCV assay kits for the Japanese clinical market.

In conclusion, we have established a Japanese reference panel for evaluation of HCV quantification assays. Using this reference panel, we found that two assay kits for HCV RNA could quantify HCV titers concordantly. We also found that the data generated by HCV core Ag assay kits correlated with the results of HCV RNA assays. However, the nominal core Ag levels measured by several kits underestimated actual levels for HCV samples with polymorphisms at aa 47 to 49 of the core Ag. The panel established in this study is expected to be useful for estimating the accuracy of currently available and upcoming HCV assay kits; such quality control is essential for clinical usage of these kits.

ACKNOWLEDGMENTS

This work was performed as part of a project for the preparation of reference panels of infectious disease specimens at the National Institute of Infectious Diseases in Japan. This work was also partly supported by grants-in-aid from the Japan Society for the Promotion of Science; the Ministry of Health, Labor and Welfare of Japan; the Ministry of Education, Culture, Sports, Science and Technology; and the Research on Health Sciences Focusing on Drug Innovation from the Japan Health Sciences Foundation.

We are grateful to Shun-ya Momose, Shigeharu Uchida, and Satoru Hino (Blood Service Headquarters, Japanese Red Cross Society) for providing specimens, to Tetsuro Suzuki (Department of Infectious Diseases, Hamamatsu University School of Medicine) for contribution to establish the reference panel, and to Kazuo Kobayashi and Masashi Tatsumi (the Committee of the Reference Panels of Infectious Disease Specimens at the National Institute of Infectious Diseases in Japan) for their helpful suggestions. We also thank the manufacturers of HCV quantification kits, including Roche Diagnostics (Tokyo, Japan), Abbott Japan (Tokyo, Japan), Fujirebio (Tokyo, Japan), Eiken Chemical (Tokyo, Japan), and Ortho Clinical Diagnostics (Tokyo, Japan), for quantification of reference panel samples.

REFERENCES

1. **Alvarez M, Planelles D, Vila E, Montoro J, Franco E.** 2004. Prolonged hepatitis C virus seroconversion in a blood donor, detected by HCV antigen test in parallel with HCV RNA. Vox Sang. 86:266–267.
2. **Aoyagi K, et al.** 1999. Development of a simple and highly sensitive enzyme immunoassay for hepatitis C virus core antigen. J. Clin. Microbiol. 37:1802–1808.
3. **Aoyagi K, et al.** 2001. Performance of a conventional enzyme immunoassay for hepatitis C virus core antigen in the early phases of hepatitis C infection. Clin. Lab. 47:119–127.
4. **Bossler A, et al.** 2011. Performance of the COBAS(R) AmpliPrep/COBAS TaqMan(R) automated system for hepatitis C virus (HCV) quantification in a multi-center comparison. J. Clin. Virol. 50:100–103.
5. **Chevaliez S, Bouvier-Alias M, Brillet R, Pawlotsky JM.** 2007. Overestimation and underestimation of hepatitis C virus RNA levels in a widely used real-time polymerase chain reaction-based method. Hepatology 46: 22–31.
6. **Elkady A, et al.** 2010. Performance of two real-time RT-PCR assays for quantitation of hepatitis C virus RNA: evaluation on HCV genotypes 1–4. J. Med. Virol. 82:1878–1888.
7. **Enomoto M, et al.** 2005. Chemiluminescence enzyme immunoassay for monitoring hepatitis C virus core protein during interferon-alpha2b and ribavirin therapy in patients with genotype 1 and high viral loads. J. Med. Virol. 77:77–82.
8. **Feld JJ, Hoofnagle JH.** 2005. Mechanism of action of interferon and ribavirin in treatment of hepatitis C. Nature 436:967–972.
9. **Feld JJ, Liang TJ.** 2006. Hepatitis C—identifying patients with progressive liver injury. Hepatology 43:S194–S206.
10. **Icardi G, et al.** 2001. Novel approach to reduce the hepatitis C virus (HCV) window period: clinical evaluation of a new enzyme-linked immunosorbent assay for HCV core antigen. J. Clin. Microbiol. 39:3110–3114.
11. **Ikeda K, et al.** 1996. Hepatitis C virus subtype 3b infection in a hospital in Japan: epidemiological study. J. Gastroenterol. 31:801–805.
12. **Kaiser T, et al.** 2008. Kinetics of hepatitis C viral RNA and HCV-antigen during dialysis sessions: evidence for differential viral load reduction on dialysis. J. Med. Virol. 80:1195–1201.
13. **Leary TP, et al.** 2006. A chemiluminescent, magnetic particle-based immunoassay for the detection of hepatitis C virus core antigen in human serum or plasma. J. Med. Virol. 78:1436–1440.
14. **Liang TJ.** 1998. Combination therapy for hepatitis C infection. N. Engl. J. Med. 339:1549–1550.
15. **Liang TJ, Rehermann B, Seeff LB, Hoofnagle JH.** 2000. Pathogenesis, natural history, treatment, and prevention of hepatitis C. Ann. Intern. Med. 132:296–305.
16. **Matsuura K, et al.** 2009. Abbott RealTime hepatitis C virus (HCV) and Roche Cobas AmpliPrep/Cobas TaqMan HCV assays for prediction of sustained virological response to pegylated interferon and ribavirin in chronic hepatitis C patients. J. Clin. Microbiol. 47:385–389.

17. **Mederacke I, et al.** 2009. Performance and clinical utility of a novel fully automated quantitative HCV-core antigen assay. J. Clin. Virol. **46**:210–215.
18. **Medici MC, et al.** 2011. Hepatitis C virus core antigen: analytical performances, correlation with viremia and potential applications of a quantitative, automated immunoassay. J. Clin. Virol. **51**:264–269.
19. **Miedouge M, et al.** 2010. Analytical evaluation of HCV core antigen and interest for HCV screening in haemodialysis patients. J. Clin. Virol. **48**: 18–21.
20. **Morota K, et al.** 2009. A new sensitive and automated chemiluminescent microparticle immunoassay for quantitative determination of hepatitis C virus core antigen. J. Virol. Methods **157**:8–14.
21. **Moscato GA, et al.** 2011. Quantitative determination of hepatitis C core antigen in therapy monitoring for chronic hepatitis C. Intervirology **54**: 61–65.
22. **Nubling CM, Unger G, Chudy M, Raia S, Lower J.** 2002. Sensitivity of HCV core antigen and HCV RNA detection in the early infection phase. Transfusion **42**:1037–1045.
23. **Ogata N, Alter HJ, Miller RH, Purcell RH.** 1991. Nucleotide sequence and mutation rate of the H strain of hepatitis C virus. Proc. Natl. Acad. Sci. U. S. A. **88**:3392–3396.
24. **Park Y, Lee JH, Kim BS, Kim DY, Han KH, Kim HS.** 2010. New automated hepatitis C virus (HCV) core antigen assay as an alternative to real-time PCR for HCV RNA quantification. J. Clin. Microbiol. **48**:2253–2256.
25. **Pawlotsky JM.** 2006. Therapy of hepatitis C: from empiricism to eradication. Hepatology **43**:S207–S220.
26. **Robertson B, et al.** 1998. Classification, nomenclature, and database development for hepatitis C virus (HCV) and related viruses: proposals for standardization. Arch. Virol. **143**:2493–2503.
27. **Ross RS, et al.** 2010. Analytical performance characteristics and clinical utility of a novel assay for total hepatitis C virus core antigen quantification. J. Clin. Microbiol. **48**:1161–1168.
28. **Saeed M, et al.** 2009. Evaluation of hepatitis C virus core antigen assays in detecting recombinant viral antigens of various genotypes. J. Clin. Microbiol. **47**:4141–4143.
29. **Seeff LB, Hoofnagle JH.** 2002. National Institutes of Health Consensus Development Conference: management of hepatitis C: 2002. Hepatology **36**:S1–S2.
30. **Takahashi M, Saito H, Higashimoto M, Atsukawa K, Ishii H.** 2005. Benefit of hepatitis C virus core antigen assay in prediction of therapeutic response to interferon and ribavirin combination therapy. J. Clin. Microbiol. **43**:186–191.
31. **Tanaka E, et al.** 2000. Evaluation of a new enzyme immunoassay for hepatitis C virus (HCV) core antigen with clinical sensitivity approximating that of genomic amplification of HCV RNA. Hepatology **32**:388–393.
32. **Tanaka Y, et al.** 2003. High stability of enzyme immunoassay for hepatitis C virus core antigen-evaluation before and after incubation at room temperature. Hepatol. Res. **26**:261–267.
33. **Vermehren J, et al.** 2008. Differences between two real-time PCR-based hepatitis C virus (HCV) assays (RealTime HCV and Cobas AmpliPrep/Cobas TaqMan) and one signal amplification assay (Versant HCV RNA 3.0) for RNA detection and quantification. J. Clin. Microbiol. **46**:3880–3891.
34. **Vermehren J, et al.** 2011. Development of a second version of the Cobas AmpliPrep/Cobas TaqMan hepatitis C virus quantitative test with improved genotype inclusivity. J. Clin. Microbiol. **49**:3309–3315.
35. **Vermehren J, et al.** 2011. Multi-center evaluation of the Abbott RealTime HCV assay for monitoring patients undergoing antiviral therapy for chronic hepatitis C. J. Clin. Virol. **52**:133–137.

Visualization and Measurement of ATP Levels in Living Cells Replicating Hepatitis C Virus Genome RNA

Tomomi Ando[1,2], Hiromi Imamura[3], Ryosuke Suzuki[1], Hideki Aizaki[1], Toshiki Watanabe[2], Takaji Wakita[1], Tetsuro Suzuki[4]*

1 Department of Virology II, National Institute of Infectious Diseases, Tokyo, Japan, **2** Graduate School of Frontier Sciences, The University of Tokyo, Tokyo, Japan, **3** The Hakubi Center and Graduate School of Biostudies, Kyoto University, Kyoto, Japan, **4** Hamamatsu University School of Medicine, Department of Infectious Diseases, Hamamatsu, Japan

Abstract

Adenosine 5′-triphosphate (ATP) is the primary energy currency of all living organisms and participates in a variety of cellular processes. Although ATP requirements during viral lifecycles have been examined in a number of studies, a method by which ATP production can be monitored in real-time, and by which ATP can be quantified in individual cells and subcellular compartments, is lacking, thereby hindering studies aimed at elucidating the precise mechanisms by which viral replication energized by ATP is controlled. In this study, we investigated the fluctuation and distribution of ATP in cells during RNA replication of the hepatitis C virus (HCV), a member of the *Flaviviridae* family. We demonstrated that cells involved in viral RNA replication actively consumed ATP, thereby reducing cytoplasmic ATP levels. Subsequently, a method to measure ATP levels at putative subcellular sites of HCV RNA replication in living cells was developed by introducing a recently-established Förster resonance energy transfer (FRET)-based ATP indicator, called ATeam, into the NS5A coding region of the HCV replicon. Using this method, we were able to observe the formation of ATP-enriched dot-like structures, which co-localize with non-structural viral proteins, within the cytoplasm of HCV-replicating cells but not in non-replicating cells. The obtained FRET signals allowed us to estimate ATP concentrations within HCV replicating cells as ~5 mM at possible replicating sites and ~1 mM at peripheral sites that did not appear to be involved in HCV replication. In contrast, cytoplasmic ATP levels in non-replicating Huh-7 cells were estimated as ~2 mM. To our knowledge, this is the first study to demonstrate changes in ATP concentration within cells during replication of the HCV genome and increased ATP levels at distinct sites within replicating cells. ATeam may be a powerful tool for the study of energy metabolism during replication of the viral genome.

Citation: Ando T, Imamura H, Suzuki R, Aizaki H, Watanabe T, et al. (2012) Visualization and Measurement of ATP Levels in Living Cells Replicating Hepatitis C Virus Genome RNA. PLoS Pathog 8(3): e1002561. doi:10.1371/journal.ppat.1002561

Editor: Andrea Gamarnik, Fundación Instituto Leloir-CONICET, Argentina

Received August 22, 2011; **Accepted** January 18, 2012; **Published** March 1, 2012

Funding: This work was supported by a grant-in-aid for Scientific Research from the Japan Society for the Promotion of Science, from the Ministry of Health, Labour and Welfare of Japan and from the Ministry of Education, Culture, Sports, Science and Technology of Japan. T.A. is a research fellow of the Japan Society for the Promotion of Science. The funders had no role in study design, data collection and analysis, decision to publish, or preparation of the manuscript.

Competing Interests: The authors have declared that no competing interests exist.

* E-mail: tesuzuki@hama-med.ac.jp

Introduction

Adenosine 5′-triphosphate (ATP) is the major energy currency of cells and is involved in a variety of cellular processes, including the virus life cycle, in which ATP-dependent reactions essential for virus multiplication are catalyzed by viral-encoded enzymes or complexes consisting of viral and host-cell proteins [1]. However, the lack of a real-time monitoring system for ATP has hindered studies aimed at elucidating the mechanisms by which cellular processes are controlled through ATP. A method for measuring ATP levels in individual living cells has recently been developed using a genetically-encoded FRET-based indicator for ATP, called ATeam, which employs the epsilon subunit of a bacterial F_0F_1-ATPase [2]. The epsilon subunit has several theoretical advantages for use as an ATP indicator; i) small size (14 kDa), ii) high specific binding to ATP, iii) ATP binding induces a global conformational change and iv) ATP hydrolysis does not occur following binding [3–5]. The affinity of ATeam for ATP can be adjusted by changing various amino acid residues in the ATP-binding domain within the subunit. ATeam has enabled researchers to examine the subcellular compartmentation of ATP as well as time-dependent changes in cellular ATP levels under various physiological conditions. For example, the ATeam-based method has been used to demonstrate that ATP levels within the mitochondrial matrix are lower than those in the cytoplasm and the nucleus [2].

Hepatitis C virus (HCV) infects 2–3% of the world population and is a major cause of chronic hepatitis, liver cirrhosis and hepatocellular carcinoma [6–8]. HCV possesses a positive-strand RNA genome and belongs to the family *Flaviviridae*. A precursor polyprotein of ~3000 amino acids is post- or co-translationally processed by both viral and host proteases into at least ten viral products. The nonstructural (NS) proteins NS3, NS4A, NS4B, NS5A and NS5B are necessary and sufficient for autonomous HCV RNA replication. These proteins form a membrane-associated replication complex (RC), in which NS5B is the RNA-dependent RNA polymerase (RdRp) responsible for copying the RNA genome of the virus during replication [9,10]. NS3, in addition to its protease activity, functions as a viral helicase capable of separating duplex RNA and DNA in reactions fuelled

Author Summary

ATP is the major energy currency of living cells. Replication of the virus genome is a physiological mechanism that is known to require energy for operations such as the synthesis of DNA or RNA and their unwinding. However, it has been difficult to comprehend how the ATP level is regulated inside single living cells where the virus replicates, since average ATP values in cell extracts have only been estimated using existing methods for ATP measurement. ATeam, which was established in 2009, is a genetically-encoded Förster resonance energy transfer (FRET)-based indicator for ATP that is composed of a small bacterial protein that specifically binds ATP sandwiched between two fluorescent proteins. In this study, by applying ATeam to the subgenomic replicon system, we have developed a method to monitor ATP at putative subcellular sites of RNA replication of the hepatitis C virus (HCV), a major human pathogen associated with liver disease, in living cells. We show here, for the first time, changes in ATP concentrations at distinct sites within cells undergoing HCV RNA replication. ATeam might open the door to understanding how regulation of ATP can affect the lifecycles of pathogens.

by ATP hydrolysis [11,12]. Consistent with other positive-strand RNA viruses, replication of HCV genomic RNA is believed to occur in membrane-bound vesicles. NS3-NS5B proteins, together with several host-cell proteins, form a membrane-associated RC. The HCV RC is localized to distinct dot-like structures within the cytoplasm of HCV replicating cells and can be detected in detergent-resistant membrane structures [13].

In this study, we first used capillary electrophoresis-time-of-flight mass spectrometry (CE-TOF MS) and the original ATeam method to determine ATP levels in cells infected with HCV or replicating HCV RNA. Using these methods, together with an ATP consumption assay, we demonstrated that ATP is actively consumed in cells in which viral RNA replicates, leading to a reduction in cytoplasmic ATP compared to parental cells. To further understand the fluctuation and distribution of ATP in HCV replicating cells, we developed a system to monitor ATP at putative subcellular sites of HCV RNA replication in single living cells by applying ATeam technology to the subgenomic replicon system. Our results show that, in viral RNA-replicating cells, ATP levels are elevated at distinct dot-like structures that may play a supportive role in HCV RNA replication, while cytoplasmic levels of ATP decrease.

Results

The concentration of ATP is reduced in HCV-infected cells

As a first approach, the concentration of adenosine nucleotides within HCV-infected and non-infected cells was quantified by CE-TOF MS analysis. ATP levels were approximately 7- and 50-fold higher, respectively, than the levels of ADP and AMP in non-infected Huh-7 cells (Figure 1A). At 9 days post-infection with HCV particles produced from a wild-type JFH-1 isolate [14], the intracellular levels of ATP, ADP and AMP were significantly (52–59%) lower than those in naïve Huh-7 cells (Figure 1A). ATP/ADP and ATP/AMP ratios were comparable among HCV-infected and non-infected cells (Figure 1B). A similar result was obtained using JFH-1/4-5 cells that harbor a HCV subgenomic replicon (SGR) RNA derived from the JFH-1 isolate [15]; the intracellular ATP level of JFH-1/4-5 cells was lower than that of parental Huh-7 cells (Figure S1). These findings are basically consistent with a recent report that phosphorylation-mediated activation of AMP-activated protein kinase is inhibited in cells undergoing HCV genome replication, and that ATP/ADP ratios are similar among cells that do and do not demonstrate HCV replication [16,17].

Measurement of ATP levels in HCV-replicating cells using ATeam

To visualize ATP levels in living cells undergoing HCV genomic replication, one of the ATeam indicators, AT1.03^{YEMK}, which has a high affinity for ATP, was introduced into HCV replicon cells carrying SGR RNA or into parental Huh-7 cells and was imaged using confocal fluorescence microscopy. Consistent with previous observations in HeLa cells [2], this ATP indicator was distributed throughout the cytoplasm. FRET signals (Venus/

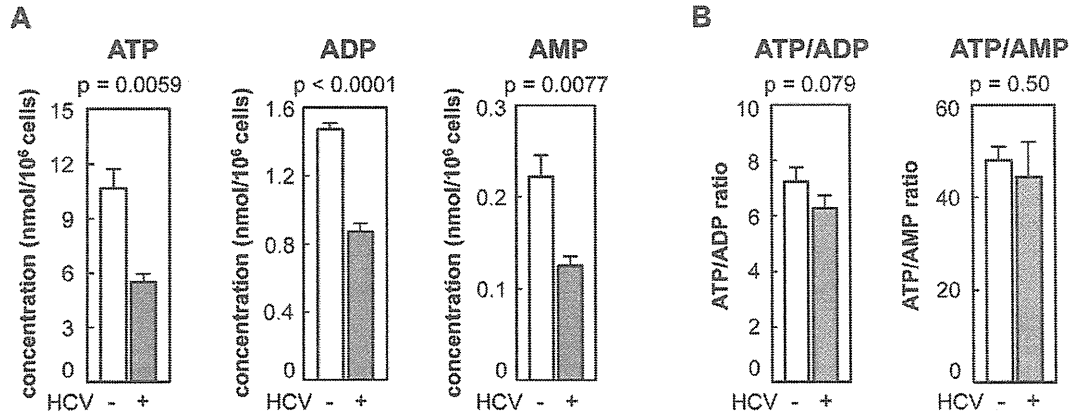

Figure 1. Levels of adenosine nucleotides in HCV-infected and non-infected Huh-7 cells determined by CE-TOF MS. (A) ATP levels were reduced in HCV-infected cells. ATP, ADP, and AMP metabolites in Huh-7 cells with (gray bars) and without (open bars) HCV infection were measured by CE-TOFMS. (B) Ratios of ATP/ADP and ATP/AMP were calculated from the results depicted in (A). All data are presented as means and standard deviation (SD) values for three independent samples. Statistical differences between HCV-infected and non-infected cells were evaluated using Student's *t*-test.
doi:10.1371/journal.ppat.1002561.g001